N73-24271

# DEVELOPMENT OF A SUPERCONDUCTING ELECTROMAGNETIC SUSPENSION AND BALANCE SYSTEM FOR DYNAMIC STABILITY STUDIES

FINAL TECHNICAL REPORT

NASA Grant No. NGR-47-005-029

Submitted to:

NASA Scientific and Technical Information Facility
P. O. Box 33
College Park, Mayland 20740



Submitted by:

R. N. Zapata

RESEARCH LABORATORIES FOR THE ENGINEERING SCIENCES

SCHOOL OF ENGINEERING AND APPLIED SCIENCE

UNIVERSITY OF VIRGINIA

CHARLOTTESVILLE

Report No. ESS-4009-101-73U

February 1973

# DEVELOPMENT OF A SUPERCONDUCTING ELECTROMAGNETIC SUSPENSION AND BALANCE SYSTEM FOR DYNAMIC STABILITY STUDIES

FINAL TECHNICAL REPORT

NASA Grant No. NGR-47-005-029

Submitted to:

NASA Scientific and Technical Information
Facility
P. O. Box 33
College Park, Maryland 20740

Submitted by:

R. N. Zapata

Department of Engineering Science and Systems
RESEARCH LABORATORIES FOR THE ENGINEERING SCIENCES
SCHOOL OF ENGINEERING AND APPLIED SCIENCE
UNIVERSITY OF VIRGINIA
CHARLOTTESVILLE, VIRGINIA

Report No. ESS-4009-101-73U

Copy No. 2

February 1973

# SECTION I

## INTRODUCTION

The Technical Annual Status Report submitted in March 1968 contained a detailed description and an analysis of the design of of a prototype superconducting magnetic suspension and balance facility for dynamic stability studies [1]. Key aspects of the evolution of the design of this unique aerodynamic testing facility were discussed in that report which was written at a time when all the main components of the facility were being built. In the three years between the publication of that technical report and the termination of the work under NASA Grant No. NGR-47-005-029, progress was reported periodically, usually accompanying requests for extensions of time and fundings, [2], [3], [4]. At the end of the funding under this grant, our research group contributed extensively to the technical program of the Second International Symposium on Electro-Magnetic Suspension, held at the University of Southampton in July 1971. The four full-length papers and two short papers we presented at the symposium represented a comprehensive and detailed review of the technical status of our project at that time [5]. Of particular relevance to the research work under this grant is the paper by this author, "The University of Virginia Superconducting Magnetic Suspension and Balance Facility," where an updated description of the facility's final design and its preliminary operating characterisitics was given.

The main section of this final technical report, which follows this introduction, consists of copies of the six papers contributed by our research group to the Southampton symposium. The final section of this report is a short discussion of progress achieved since the termination of this grant (with NASA support under grant NGR-47-005-112) which is directly relevant to the main questions left unanawered in Zapata's second symposium paper.

## SECTION II

## TECHNICAL REPORT

1. "The University of Virginia Superconducting Suspension and Balance Facility," R. N. Zapata.

2. "The Use of Superconductivity in Magnetic Balance Design," F. E. Moss.

3. "Data Acquisition and Reduction for the UVA Superconducting Magnetic Suspension and Balance Facility," I. D. Jacobson, et al.

4. "The Use of Iron and Extended Applications of the U. Va. Cold Balance Wind Tunnel System," H. M. Parker, J. R. Jancaitis.

5. "Electromagnetic Position Sensor for a Magnetically Supported Model in a Wind Tunnel," W. R. Towler.

6. "Safety Aspects of Superconducting Magnetic Suspension Systems," R. N. Zapata.

# THE UNIVERSITY OF VIRGINIA SUPERCONDUCTING MAGNETIC SUSPENSION AND BALANCE FACILITY*

by

Ricardo N. Zapata
University of Virginia
Department of Aerospace Engineering and Engineering Physics
Charlottesville, Virginia USA

## ABSTRACT

A prototype facility comprising a superconducting magnetic suspension and balance and a supersonic wind tunnel has been developed with the objectives of (1) establishing the feasibility of applying the 3-component magnetic balance concept to dynamic stability studies, and (2) investigating design concepts and parameters that are critical for extrapolation to large-scale systems. Many important design and operational aspects as well as safety considerations are dictated by the cryogenic nature of this advanced-technology facility. Results of initial tests demonstrate that superconductors can be utilized safely and efficiently for wind tunnel magnetic suspensions. At the present stage of development of this facility, controlled one-dimensional support of a spherical model has been achieved.

*Work supported under NASA Grants NGR-47-005-029, NGR-47-005-110, and NGR-47-005-112

## I - INTRODUCTION

The concept of a "cold" magnetic balance was first advanced by H. M. Parker at the first international Symposium on Magnetic Wind Tunnel Model Suspension and Balance Systems in 1966.[1] There he discussed scaling laws for normal conductor coils and presented convincing arguments in favor of a proposed magnetic suspension operating at 20°K. The subject of possible applications of superconducting technology to wind tunnel magnetic balance systems was discussed with considerable interest in a special session; a review of the then current status of superconductor technology and subsequent discussion sparked by key questions brought up by potential users, revealed the inadequacy of knowledge on this topic available at that time and provided no definite encouragement to those potential users. Another topic which received much attention at the first symposium was the application of magnetic suspension techniques to dynamic stability studies. Two research groups presented discussions on this topic based on actual experience with five-component balances. The advantages and limitations of three-component balances were debated in a more speculative vein since no operational experience was available then.

Against this background, in early 1967, a University of Virginia team, with the financial backing of NASA's Langley Research Center, launched efforts to build a cryogenic magnetic balance prototype facility with the stated objectives of (1) establishing the feasibility of applying the 3-component balance concept to dynamic stability studies; (2) investigating design concepts and parameters that are critical for extrapolation to large scale facilities. These efforts have been largely successful although the complete prototype facility has not attained operational status yet. As with most state-of-the-art projects the road to success has been longer and more arduous than originally anticipated, with many forced detours and waiting periods along the way. There is much progress to report, however, and this second international symposium on electromagnetic suspension presents a timely forum for it. This paper will discuss the evolution of the prototype magnetic suspension facility with special emphasis on critical design concepts, fabrication and operational problems, and current operational status. Three additional papers contributed by members of the U.Va. research team will explore in more detail the most significant contributions of this project to the technology of wind tunnel magnetic suspension and balance systems.[2,3,4]

## II - DESIGN CONSIDERATIONS

The design of the Superconducting Magnetic Suspension and Balance (SMSB) facility has undergone substantial evolution since the project was launched in 1967. For the most part this evolution is due to increased knowledge about the different technologies employed in this rather complex system. In some cases, it has not been so much a question of becoming sufficiently familiar with the relevant subtleties of an established technology as it has been a question of trying to keep pace with relevant changes of a rapidly evolving technology. In other cases, unanticipated state-of-the-art limitations of a given technology had to be recognized and accepted. Throughout this process, the two essential objectives of this project listed in the previous section, have been kept as a point of reference to establish priorities among design criteria. For example, the working-prototype function is emphasized over the research-facility function. To meet the first objective, an aerodynamic simulation facility (wind tunnel) and a three-component electromagnetic suspension and balance are required. The wind tunnel must be capable of producing steady state flow of known description for a length of time sufficient to effect controlled magnetic support of a model and acquire dynamic stability data. The

balance must be capable of holding the model to a fixed wind tunnel position on the average, within reasonable limits of magnet size and power dissipation, and measuring the magnetic forces acting on the model at all times.

The second objective suggests two guidelines for the choice of solutions to individual design problems. First, whenever technically and economically feasible, a more sophisticated solution than absolutely needed for the prototype facility should be chosen if it represents the most likely solution for large-scale facilities. Second, problems that are peculiar to the prototype facility, but not likely to arise in large-scale facilities, should be deemphasized whenever possible. Finally, it is appropriate to recognize time as an ever-present constraint, permeating the decision-making process at all levels.

In the remainder of this section, the above considerations will be illustrated with concrete examples as the most significant aspects of the design evolution of this prototype magnetic balance are discussed in some detail. For the sake of clarity each subsystem will be discussed separately, although it should be obvious that many important design decisions are based on the interactions of these subsystems. These interactions are schematically represented in the block diagram sketched below.

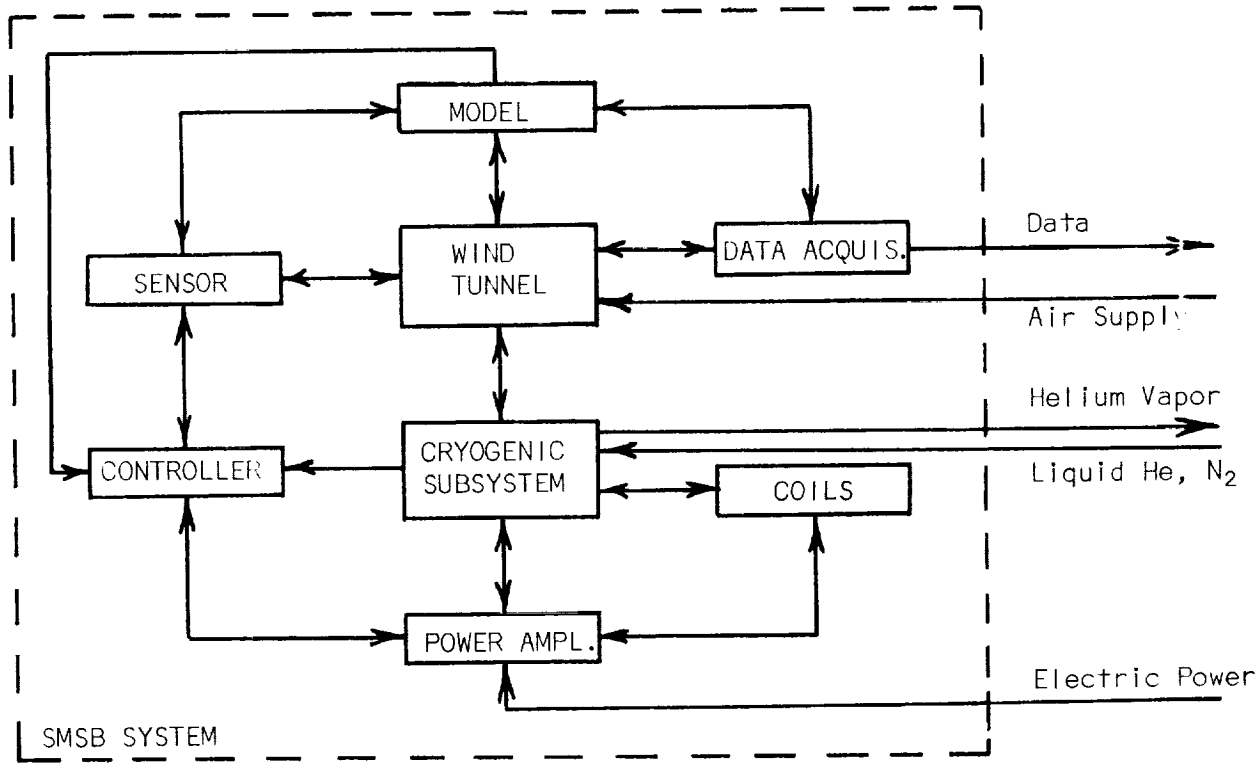


(1) The Wind Tunnel

The cryogenic nature of the electromagnetic balance and the symmetry of the coil configuration suggested a vertical, axisymmetric wind tunnel early in the design process. The overall scale of the SMSB facility was set by the arbitrarily selected dimension of the wind tunnel test section: 6-inch diameter. This relatively small dimension practically dictates the choice of a supersonic over a subsonic facility if meaningful simulation of free flight is desired. Combining the available capability of the power plant with a 2000 cu. ft. air storage capacity, a Mach 3 tunnel operated in a blow-down mode with atmospheric discharge can be run for approximately five minutes. To obtain this length of run time it was necessary to

optimize the internal geometry of the wind tunnel to improve the efficiency of the supersonic diffuser. A fixed annulus and a movable centerbody form a variable area second throat, while at the same time providing a convenient support for the mechanical holder needed during the transients at the beginning and at the end of a run. These tunnel elements have been drawn to scale in Figure 1, together with the stagnation chamber, the contoured nozzle, and the subsonic diffuser. For details of the tunnel optimization process see reference 5. Representative results will be shown in the section on current status.

(2) The Coil Subsystem

In the basic magnetic suspension originally proposed by Parker,[1] an isotropic, ferromagnetic sphere is uniformly magnetized when placed in a uniform magnetic field. Forces are exerted on the sphere by pure magnetic field gradients produced by pairs of coils, with a common symmetry axis, placed symmetrically about the sphere, and with equal but opposite currents. Direction and magnitude of these forces depend on the angle between the gradient coil axis and the direction of magnetization of the sphere. Two special coil configurations, yielding sets of orthogonal forces, are particularly attractive for application to vertical wind-tunnel balances: the $\tan^{-1}\sqrt{2}$ configuration produces forces aligned with the vertical axis and two perpendicular axes on a horizontal plane; the $\tan^{-1}\sqrt{8}$ configuration produces forces aligned with the sides of a cube whose diagonal coincides with the vertical axis. The latter configuration was adopted for the SMSB facility because its high degree of symmetry tends to optimize the utilization of space around the wind tunnel, thus resulting in higher efficiency of the coil system. In this case, the basic $\tan^{-1}\sqrt{8}$ configuration has been supplemented by an additional pair of gradient coils whose symmetry axis coincides with the tunnel axis, to balance the average drag force on the suspended model. The magnetizing Main Field (MF) coil and the two Drag Augmentation (DA) coils operate in a d.c. mode. The six Gradient (G) coils, needed for stability in all directions, operate in an unsteady, or a.c., mode. Originally, all coils were to be made of high-purity aluminum and operated at 20°K. Uncertainties about the performance of supercooled coils and the realization that it would be impractical to use supercooled coils in large-scale facilities, prompted the decision to switch to superconducting coils. The fabrication and the operation of the MF coil and the DA coils are straightforward applications of modern superconductivity technology, while uncertainties associated with the operational performance of the G coils were responsible for uncertainty about the eventual success of this entire magnetic balance concept, until recently. Critical questions on stability of superconductors and heat dissipation resulting from a.c. operation had to be answered. The paper by F. E. Moss[2] in the symposium discusses these issues in detail. Suffice it to say here that the G-coils currently in use represent a second-generation design utilizing the best superconductors commercially available at the present time; current developments in applied superconductivity show promise that superconductors with much improved a.c. characteristics will be available before long.

All coils are wound on fiberglass-epoxy forms of special design. The MF coil and the DA coils were fabricated by Atomics International of Canoga Park, California. The 6 G coils have been wound in-house; a simple technique has been developed to detect the presence of shorts along the edges of the windings, an ever-present possibility given the geometry of the superconductor and the small thickness of the insulating tape. The entire coil assembly forms a structure capable of withstanding the large inter-coil forces internally. This is an important consideration in a cryogenic coil system. A scale sketch of this system is shown in Figure 2. The principal

design and operational characteristics of each type of coil are summarized in Table I. The magnitudes of the axial magnetic field and of the axial magnetic field gradient due to the MF coils and the DA coils are plotted as a function of axial distance in Figure 3.

(3) The Cryogenic Subsystem

The requirement of providing a liquid helium environment for the operation of the superconducting coils is satisfied by a cryogenic subsystem consisting of three principal components: a helium cryostat, a set of vapor-cooled current leads, and appropriate pressure and temperature instrumentation. This cryogenic subsystem is the least conventional component of the SMSB facility and has, at the same time, influenced the design of several other components quite markedly. For this reason, it is appropriate that the following discussion be sufficiently comprehensive even at the risk of making it somewhat lengthy.

Experimental helium cryostats must meet the basic specification for a storage dewar, i.e., hold a prescribed quantity of liquid helium with minimum refrigeration losses that occur chiefly by conduction and radiation mechanisms. Conduction losses are minimized by (a) constructing the cryogenic vessel with thin, low thermal-conductivity materials, (b) surrounding the liquid container with a hard-vacuum jacket, and (c) careful design of leads and internal supports connecting low and high temperature regions. Radiation losses are minimized by either of two methods: (1) surrounding the liquid container with a wall held at an intermediate temperature (typically, liquid nitrogen temperature), (2) interposing a series of reflecting surfaces or shields between the liquid container wall and the (room temperature) outside wall; often a combination of both these methods is used for increased effectiveness.

Aside from the foregoing specification, the SMSB cryogenic unit must satisfy the following functional constraints: i) room temperature access for the supersonic wind tunnel, the model position sensor, and other system components must be provided, ii) the distance between the coils and the wind tunnel should be kept as short as possible, iii) interference with the magnetic interaction between the coils and the suspended model must be avoided, iv) accessibility to the coils and other components inside the dewar must be reasonably good. Finally, a common specification for experimental systems, high reliability, assumes special importance in this case.

Without going into excessive detail, consider a few of the most significant consequences of these specifications. For example, constraint (i) leads to a generalized annular geometry in potential conflict with constraints (ii) and (iii), since the inside walls of the annulus will stand between the coils and the suspended model. Futhermore, the possibility of using a simple radiation barrier around the helium container (typically, a copper skirt held at liquid nitrogen temperature, located inside a single vacuum jacket), is eliminated since the eddy currents induced in such a high thermal-(and electrical-) conductivity barrier will surely interfere with the interaction between the coils and the model. An alternate solution consisting of packing superinsulation (aluminized mylar) in the vacuum jacket surrounding the helium vessel has to be eliminated for the same reason. The only remaining practical solution uses a liquid-nitrogen radiation shield; however, this solution increases considerably the complexity of the design of the cryostat, since it requires four walls between the liquid helium environment and the room temperature environment. This solution is still in potential conflict with constraints (ii) and (iii) as can be appreciated upon examination of Figure 2. The cylindrical inner walls of this cryostat (shown as vertical lines in the figure) are very thin

and are spaced very closely to one another in an effort to meet constraint (ii). Originally, all four inner tubes were made of fiberglass-epoxy bonded to the rest of the cryogenic vessel by a special process. It must be remembered at this point that the effectiveness of a liquid helium dewar depends most critically on the tightness of the vacuum jacket surrounding the liquid container. Even small leaks (by more conventional standards) cannot be tolerated. At the same time, the success fo this entire electromagnetic balance concept hinges upon the ability to operate the balance without excessive helium losses. Consequently, when a vacuum leak developed in one of the fiberglass tubes of the inner vacuum jacket, and resisted all attempts to repair it, both tubes of that vacuum jacket were replaced by non-magnetic stainless steel tubes. Experiments conducted to determine the nature and magnitude of the effect of the presence of these (metal) walls on the magnetic interaction between the coils and the model, revealed that magnetic field attenuation and phase shift associated with eddy currents induced in these walls, were of small but finite magnitude. As expected, these effects are accentuated as the frequency of the coil current increases. These experiments are documented in reference 6.

The dewar is physically separable into two parts: the inner, or liquid helium dewar, and the outer, or liquid nitrogen dewar. this characteristic proved invaluable at the time the lead in the inner dewar was detected and subsequently fixed. Unless there is a reason to separate them, normally both parts stay together when the coil assembly is removed from the system. When the system is fully assembled, both these parts are independently fastened to the top plate that supports the entire assembly (see Figure 2).

A set of 10 current leads carries electric current from the outside of the dewar to the nine coils inside. These leads are specially designed to use the cooling power of helium vapor to maximum advantage by serving as outlets for the helium boil-off. One such vapor-cooled lead is shown in Figure 2. In principle, for every current distribution in the coil system there is an optimum distribution of helium vapor flow rate through the vapor-cooled leads that minimizes the total helium boil-off in the dewar.

In practice, if the leads are adequately sized, it is not necessary to monitor the vapor flow distribution, but it is only necessary to monitor the temperature of the outflowing vapor to detect gross unbalances indicative of severe malfunctions. In the SMSB facility all vapor-cooled leads are equipped with thermocouples at the ends leading out of the dewar; in addition, all connecting tubes between the leads and the helium recovery manifold are individually valved to facilitate any necessary adjustments. The details of the design of the vapor-cooled leads can be found in a publication by Efferson[7] from which all the information needed to fabricate the leads for this facility was obtained.

The instrumentation requirements for the cyrogenic subsystem are better understood by considering some of its key operational aspects. For example, since liquid helium is considerably more expensive than liquid nitrogen, it is common practice, specially when large systems are involved, to pre-cool the system to liquid nitrogen temperature before starting the transfer of liquid helium into the system. This pre-cooling process can be accelerated by bleeding dry gas into the vacuum jacket between the liquid helium and liquid nitrogen containers until the pressure reaches several torr. It is clear that pressure and temperature instrumentation requirements result from the need to perform the pre-cooling operation. Additional requirements result from the need to determine liquid level during liquid helium transfer and during the performance of a test.

Conventional vacuum gauges are adequate for measuring all working

pressure levels between atmospheric pressure and the ultimate vacuum (about $10^{-4}$ torr) achieved in the jackets surrounding the nitrogen and the helium dewars. Temperature information is needed at three specific temperature levels: (1) room temperature, as a reference for the measurement of coil parameters (R,L,Q), (2) liquid nitrogen temperature, as an indicator of the state of readiness of the pre-cooling process, (3) liquid helium temperature as an indicator of coverage by liquid helium during transfer. Miniature carbon resistors are installed at five locations, marked with an x in Figure 2, between the lower surface of the bottom coil and the first radiation shield above the coil assembly. These resistors are bonded to large mases (for example, the flange of a DA coil) so as to insure that their temperature reflects that of a given part of the coil assembly rather than being dictated by local heat transfer conditions. Furthermore, their operating current is minimal. The output circuit has been arranged so as to produce calibrated readings of the three temperatures of interest at conspicuous points on the readout scale. No practical meaning is attached to readings at intermediate points.

In addition to the temperature sensors, a set of five liquid-level sensors are located at nearby locations. These are particularly useful during the balance tests as the level of liquid helium descends, but uncovered portions of the coil assembly remain at essentially liquid helium temperature. The liquid-level sensors are carbon resistors similar to the temperature sensors, but they are installed so as to be thermally isolated from large masses. Furthermore, a relatively large current is constantly circulated through them. As these sensors become uncovered their temperature rises substantially above that of liquid helium. Their output circuit uses a very effective sound alarm system as a readout.

The basic instrumentation set of the cryogenic subsystem is completed with a gas flowmeter connected in the main line of the manifold that collects the output from all vapor-cooled leads in the system. The basic function of this instrument is to provide a rough indication of the total instantaneous helium boil-off rate inside the cryostat, mostly as a safety warning of coil malfunction.

(4) Model Position Sensing

There are three separate requirements for model position information during a successful run of the SMSB facility. These are: (a) the operator of the facility needs to see the model for proper coordination of the launching and recapturing maneuvers, (b) an error signal is needed to close the automatic control loop effecting stable model support, (c) position and attitude coordinates, as functions of time, constitute the model "trajectory" information needed as data to compute the desired aerodynamics parameters.

The practical difficulties of establishing a direct optical path between a suspended model and an outside observer should be apparent upon reexamination of Figure 2. The many optical elements necessary to bend the light rays around the dewar become relatively inaccessible for modifications and for fine adjustments. Moreover, the annular space between the dewar and the wind tunnel, where any type of model position detector must be installed, should not be made larger than strictly necessary because as the thickness of this annulus grows so does the distance between the coils and the model (constraint (ii) in the previous section).

Fortunately, requirement (a) can be satisfied with a relatively low resolution system. A first-generation optical monitor which combines lenses, mirrors, and fiber optics conduits has been built and tested successfully.

The key components are a wide-angle lens with a field of view of approximately 10 cm at the plane of the tunnel axis, a length of coherent fiber optics, and a closed-circuit television monitor. For details about this optical system, see reference 8.*

Requirements (b) and (c) demand high resolution systems. Traditionally error signals for magnetic balance control loops have been obtained from optical detectors employing different combinations of light beams, photocells, and other components. These detectors are relatively simple to operate and have built a good record of reliability. Their one important disadvantage is that they must be tailored to a given model. This inconvenience in addition to the difficulties peculiar to this facility outlined above, made us look with favor on the development of an electromagnetic position sensor by the MIT magnetic suspension group. This type of sensor operates on the principle of the differential transformer; its key advantages from our point of view, are: (1) one sensor can be used for different models with no modifications required, (2) the spacial distribution of the sensing elements lends itself admirably to the tight space available in our facility. A paper by T. Stephens, MIT, will discuss this sensor in detail later in this symposium.[9] Suffice it to say here that we have encountered serious difficulties while attempting to integrate this type of sensor with the rest of the SMSB facility, in the form of high amplitude noise originating from the periodic switching process of the power amplifiers. Time has not permitted to establish conclusively whether there is a basic incompatibility between the power amplifiers and this type of sensor, or whether appropriate modifications of the circuitry will help overcome the present impasse.

Presently, the development of the facility is proceeding with an optical model position detector in the feedback control loop. A rather crude optical system was built in the interest of saving time in the primary development of the superconducting balance.** The principal design specification for this temporary sensor is compatibility with adjacent elements of the system position control loop. If the problems encountered with the electromagnetic sensor are not resolved satisfactorily, a highly sophisticated optical sensor, presently in the preliminary design stage, will be required for the complete facility.

Finally, concerning requirement (c), the whole subject of data acquisition and reduction for this facility will be discussed in detail in a paper by I. D. Jacobson et al., in this symposium.[3]

(5) The Control Subsystem

The basic function of the control subsystem is to obtain information about the position of the magnetically suspended model, compare this information with the specified model position, and command the power amplifiers to take appropriate remedial action. The manner in which this function is performed can have profound influence on the dynamic behavior of all other elements of the magnetic suspension system. Conversely, the dynamic characteristics of these other elements must be known before detailed design decisions with regard to the control subsystem can be made. The interactive nature of the operation of a magnetic suspension system is illustrated in the functional diagram shown in Figure 4. For the purposes of this discussion, all blocks between the POSITION SENSOR block and the POWER AMPLIFIER blocks are taken as part of the control subsystem.

---

* A schematic of this device is shown as Figure 3 in paper K, this symposium.

** A schematic of this optical sensor is shown as Figure 1 in paper K, this symposium proceedings.

Both types of model position sensors constructed for the SMSB facility produce output signals of a few volts d.c. for displacements on the order of 25 millimeter. The basic sensitivities of the 3 sensing channels are in general dissimilar and not adequate for direct use by the controller. Consequently, the raw signals from the sensor are first processed by the STATIC POSITION CONTROL element, where the sensitivities are brought to the proper, equal level by means of variable gain adjustments. Next, it is necessary to transform the signals from a wind-tunnel coordinate system to a coil coordinate system. Recall that in the $\tan^{-1}\sqrt{8}$ coil configuration the directions of the orthogonal forces produced by the 3 G coil pairs (x',z',y') do not coincide with the conventional wind tunnel axes (x,y,z) but are instead distributed symmetrically about the principal axis of the vertical wind tunnel. The transformation of axes is accomplished by the SENSOR COORDINATE TRANSFORMATION element based on the transformation matrix:

$$\begin{pmatrix} x' \\ y' \\ z' \end{pmatrix} = \begin{pmatrix} 0.577 & 0.577 & 0.577 \\ 0.577 & -0.788 & 0.211 \\ 0.577 & 0.211 & -0.788 \end{pmatrix} \begin{pmatrix} x \\ y \\ z \end{pmatrix}$$

A similar element is available to process perturbation inputs to the suspended model, more naturally introduced in the tunnel coordinate system.

Operation of the SMSB facility will provide quasi-six-degrees-of freedom simulation capability for dynamic stability studies. A key point in this simulation concept is that, above a given frequency, the model should be free to undergo oscillatory motion without being "hunted" by the magnetic suspension. This extra freedom is achieved by including ADJUSTABLE LOW-PASS FILTER elements in the control subsystem. The available range of cut-off frequencies is 5, 10, 15 and 30 Hz.

The CONTROLLER is the brain of the control subsystem. Usual design specifications include simplicity, speed of response, stability and linear mode of operation for small disturbances. To these, a high-priority design criterion must be added in this case, i.e., minimum a.c. losses in the superconducting coils. This last requirement has been translated into designing a system with no overshoot for a step change in displacement. Moreover, the (open-loop) minimum-energy control system has been used as a reference for evaluating the relative merits of other (closed-loop) possible control systems vis-a-vis the high-priority design criterion.

All of the above requirements point to a dual-mode control configuration. For small displacements the system should be linear; for larger displacements the system is a minimum-time control system which returns itself to the linear mode. The estimated coil a.c. losses associated with this control configuration are only moderately larger than the corresponding losses associated with a minimum-energy control configuration. In this sense, the controller can be called quasi-optimal.

Each channel of the magnetic suspension is actually a third order system. the construction of a third-order minimum-time controller would have been a very difficult task. However, since the power amplifier - coil combination is very fast, the system was considered to be second order for the design of the control law, and subsequently corrections were included to account for the fact that current changes need non-zero times. A schematic diagram of the controller is shown in Figure 5.

(6) Power Supplies

Design specifications for the energy sources needed to power the different types of coils in the SMSB facility are vastly different, ranging from the simple requirements for the strictly d.c. operation of the Main Field

coil to the state-of-the-art requirements for the unsteady operation of the Gradient coils. Separate discussions for each type of energy source follow.

(a) Main Field Power Supply: The MF coil must be energized with a constant-current power supply to maintain a steady magnetizing field. Modest voltage capability is required to overcome lead and connection voltage drops and to charge the coil to rated current (nominally, 100 A) in a reasonable length of time (typically, of the order of one minute), by manual operation. These requirements, plus normal reliability and economy criteria, are satisfied by a BECKMAN INSTRUMENTS MODEL C-25-100 constant-current saturable reactor type power supply, which employs no active devices other than solid state rectifiers. Current control is effected by an adjustable autotransformer making the power supply reliable and rugged.

A very important consideration in the design of the main field circuit is the amount of energy stored in the coil at rated current:

$$W = 1/2\ LJ^2 = 2.55 \times 10^4 \text{ Joules}$$

In the event of a failure in some part of the circuit tending to stop or drastically decrease the current, the reverse voltage applied by the coil, if not controlled, could damage the coil and the power supply. The resulting helium boil-off is a potential safety hazard not to be taken lightly. To prevent the sudden release of energy a high-current silicon rectifier has been connected (reverse biased normally) across the coil terminals outside the dewar. This prevents the reverse voltage from exceeding the diode drop (about 1 Volt). Furthermore, this diode and its lead resistance permit a faster shutdown of the Main Field coil under normal operating conditions.

(b) Drag Augmentation Power Supply: Inasmuch as the function of the Drag Augmentation coil is to balance the steady-state component of the aerodynamic drag minus the model weight, the operational mode for these coils must be described as slowly adjustable d.c., with an anticipated response-time requirement on the order of a few seconds. This operational capability, permitting the average Gradient coil current to remain at a steady level for maximum range, can be achieved with a voltage-controlled current source. The model vertical position sensor and proper compensation comprise the remainder of the drag-augmentation control loop.

A Hewlett-Packard, Harrison Division Model 6472A voltage-controlled current source (0-64 VDC, 0-150A), with provision for manual or remode programming was chosen. The upper voltage limit of 64 volts is capable of producing a response on the order of:

$$\Delta t = L\Delta i/E_{max} = 20 \text{ seconds}$$

for a current change of 0 to 100 A through the combined inductance of 12.4 henries of the DA coil pair. A spark gap across the power supply terminals will be installed as a safety protection against sudden decreases in coil current, for reasons similar to those discussed in the previous sub-section.

(c) Gradient Coil Power Amplifiers: The most challenging specification for the power amplifiers that drive the Gradient coils is that they must effect large current changes in short times through almost purely inductive loads. Furthermore, the required current changes must be produced with no overshoot and with minimum energy dissipation at the load. The load in this case consists of a pair of G coils, connected in series, with a total inductance of approximately 8 H. Power losses in the Gradient-coil system are confined to a.c. losses in the coils, lead and connection resistances,

and internal power amplifier losses. The maximum current change specified is from 0 to 350 A in a time interval the order of 16 msec.

Amplifiers meeting the foregoing requirements were not commercially available at the time (1968) the set of specifications was completed. The amplifiers presently used in the SMSB facility were developed especially for this facility by the Brown Boveri Corporation, Oerlikon Engineering Division, Zurich, Switzerland. They are designed to provide from 8 A to 350 A to the coil load in accordance with a voltage control signal, at a maximum rate of current increase of 25 A/msec. The static transfer characteristic is linear. The amplifiers will follow a sine wave input from d.c. to 30 Hz with no appreciable drop in amplitude over the full current swing; above 30 Hz the frequency response is a function of the current amplitude. Maximum working frequency is 300 Hz, although at that frequency the response at full current demand is only 10% of full amplitude.

The power amplifiers operate from 480-volt 3-phase mains and utilize an intermediate current and voltage regulated 210 volt d.c. power supply to charge a large (0.12 Farad) capacitor bank. After the initial charging of the capacitors upon turn-on, the d.c. power supply is only required to supply the charge necessary to compensate for losses in the system, i.e., when the coil current is increased, the capacitors supply energy and when the current is decreased, energy is returned to the capacitors minus losses. Current changes are effected by a switching circuit employing thyristors and diodes. The usual problems associated with turning thyristors off (current overshoot) and thyristors dead time (high driving voltage requirement) are eliminated by the insertion of the intermediate d.c. supply.

A simplified schematic of a power amplifier is shown in Figure 6, where L8 represents a G-coil pair, A9 and A14 are load thyristors, A8 and A15 are recharging thyristors, A10 and A13 are free-wheeling diodes, and C is the energy-storage capacitor bank. Three modes of operation result from turning off a single or both load thyristors:

(i) Both A9 and A14 are conducting; full positive voltage (210 V) is applied across L8 producing maximum rate of current increase (25 A/msec).

(ii) One load thyristor, for example A9, is turned off when A8 is fired, resulting in an exponential current decrease as it flows through A10 and A14. This is a coasting mode induced by a constant or slow changing demand.

(iii) Both A9 and A14 are turned off by fixing A8 and A15; full negative voltage (-210 V) is applied across L8 producing maximum rate of current decrease (-25 A/msec) through A10 and A13.

When a voltage step is applied to the control input, the current increases at maximum rate until the value is 8 A above the required value. At this point the amplifier goes into a coasting mode, and the current decreases until it reaches a value 8 A below the required value. Then the amplifier goes into the maximum rate of increase mode again until the current is again 8 A higher than required. This cycle is repeated until the control input is changed. An analogous process takes place when a current decrease is demanded by applying a negative voltage step to the control input. Figure 7a, showing a tracing from an oscilloscope photograph of the current response to an applied square wave input, illustrates the three modes of operation of the amplifier. The current response to an applied sine wave input is shown in Figure 7b.

A fundamental aspect of the design of these power amplifiers is safety, primarily with regard to the operation of the superconducting Gradient coils.

Although the magnetic field energy associated with the d.c. operation of the coils is substantially lower than the energy stored by the Main Field coil, it is nevertheless considerable (500 joules per G-coil pair). Furthermore, the a.c. operation of the coils can lead to high energy dissipation if transition to a normal conduction mode occurs. In such cases, the current should be decreased to zero as quickly as possible. Protection from damage to the power amplifiers resulting from coil malfunction is also of greater concern here than it is in the case of the power supplies for the d.c. coils, simply because these power amplifiers cannot be replaced readily.

An elaborate system of protective interlocks was incorporated as an integral part of the operating circuits of the amplifiers. These safety devices prevent operation of the amplifiers unless, for example, adequate voltages and adequate cooling are available for proper functioning of all components. At the same time, excessive energy dissipation, whether it originates in the load or internally, will shut the amplifiers off promptly. This safety feature has proven very effective and reliable every time a Gradient coil failure has occurred. In fact, the amplifier will cut off before the operator can detect an anomalous increase in the flowmeter reading.

## III - OPERATIONAL CONSIDERATIONS

Many of the important operational characteristics of the SMSB facility are typical of most magnetic wind-tunnel suspensions and will not be discussed in this paper. Only those aspects of the operation of this facility that are peculiar to its cryogenic nature will be commented on briefly. Three, clearly interrelated, such aspects are considered here: time scales, operating costs, and safety.

### (1) Time Scales

The SMSB facility cannot be simply turned on or off at the flip of a switch. At the present level of operational expertise (8 full tests), it takes approximately 48 hours from the time the facility is fully assembled to the time current can be supplied to any of the coils. Most of this interval is needed to pre-cool the inner components of the facility to liquid-nitrogen temperature, in the interest of saving liquid helium. Typically, preparations for a test are started in mid-morning of day 1 by evacuating both vacuum jackets and bleeding dry helium gas at room temperature into the helium dewar through the vapor-cooled leads. Next, the first charge of liquid nitrogen is fed into the appropriate cryostat chamber. Liquid nitrogen continues to be fed into the cryostat at a rate necessary to keep the level of liquid nitrogen near the top of the cryostat; this is largely an automatic process continuing through day 2. Pre-cooling is completed early in day 3.

Liquid helium transfer takes approximately 2 hours under normal conditions. An additional 30 minutes interval is needed to allow for proper settlement of the liquid-helium level and to measure this level with a dip stick. The system is thus ready for testing by mid-morning of day 3.

Time is also important during a test. Basic, steady-state refrigeration losses under no-load conditions amount to approximately 4 liters of liquid helium per hour. A normal charge of liquid helium includes approximately 80 liters available for consumption during the test, the rest being necessary to maintain minimum coil-coverage level. Thus, experiments must be well planned in advance to minimize idle time. When the facility becomes routinely operational the duty cycle will be of the order of 5 minutes of aerodynamic testing every 2 hours, the intervening time being essentially a waiting period needed to replentish the high pressure air storage tanks. Assuming efficient planning for optimum utilization of testing opportunities,

6 five-minute aerodynamic runs can be performed in a 10-hour period with a single charge of liquid helium.

The foregoing discussion is concerned with normal operation of the SMSB facility after it has been fully developed; the time scale involved is short, in the sense that one test run is involved. During the facility developmental period, a much longer time scale, determined by the time between test runs, is of perhaps greater importance than the short time scale, particularly in the final stages of facility development. The two scales are not independent of each other, however, since characteristic times in the long-time scale are dictated mostly by economic considerations that depend very strongly on short-time scale factors. Unless unlimited resources (man power, liquid helium) are available, a practical figure for frequency of testing is 1 test per month. Even if this figure could be doubled, it is easy to see that the traditional approach for "debugging" system components and testing ideas and solutions for typical developmental problems cannot be used in this case. Every test becomes necessarily a major test; a good idea based on results of today's test cannot, in general, be tried tomorrow, but rather in 3 weeks or a month.

Clearly, the long-time scale is undesirable since it makes it difficult to maintain continuity of effort and tends to delay progress significantly. In an effort to overcome these difficulties, the feasibility of building an auxiliary coil system using conventional conductors operating at reduced currents furnished by the regular facility power supplies, and compatible with the other components of the SMSB facility, is being investigated.

(2) Operational Costs

Cost of cryogenic fluids varies drastically depending on factors such as total rate of consumption and geographic location of consumers relative to that of suppliers. Consequently, the figures given below are representative only in the restricted sense that they correspond to actual rather than estimated expenditures.

Normally, about 300 liters of liquid helium are used to fully charge the cryostat (up to the level of the bottom radiation shield in Figure 2). After 6 to 10 hours of testing (depending on the nature of the tests, a.c. losses can vary substantially), 80 liters can be recovered in liquid form and returned to the supplier, for a total net consumption of 220 liters. For the same test, liquid nitrogen consumption totals 1400 liters, divided as follows: 1200 liters for pre-cooling and 200 liters during the test. Thus:

| | |
|---|---|
| 220 liters liquid He @ $4.50 | $990 |
| 1400 liters liquid He @ $0.10 | $140 |
| Total cost of cryogenic fluids | $1130 |

Finally, the price of liquid helium quoted above is based on full recovery of the helium gas evolving from the cryostat. This recovery is effected by connecting the downstream end of the flowmeter to a recovery line which runs to the storage facility of the helium liquefaction plant (about one-half mile away).

(3) Safety

It should be reasonably obvious that the operation of the SMSB facility involves higher-than-ordinary potential safety hazards. The combination of large quantities of liquid helium and high energies stored in the magnetic field is awesome. In response to this inherent risk, all energy sources have been protected against sudden release of this magnetic field energy into the cryostat. This was discussed in some detail in the section on Power Supplies. The effectiveness of the protective devices was demonstrated

quite dramatically when coil failures occurred at several stages in the development of the facility. These failures included mechanical destruction of one DA-coil, mild shorting of windings in two different G coils, and severe shorting of windings resulting in gross localized damage to the windings of one G coil. In all but one of these failures the damage was confined to a small region in the coil that failed. The one exception was the mechanical failure of the DA-coil. No protective spark gap had been yet installed across the terminals of the power supply, with the result that the voltage control amplifier was damaged by the back emf from the suddenly opened coil. However, no damage to the cryostat resulted, even though for a brief time the helium boil-off rate, as indicated by the flowmeter, reached very high values. This transient excessive boil-off rate was recorded also by the top liquid level indicator, which sounded the alarm as it became temporarily uncovered by liquid.

In summary, the SMSB system can be operated safely by virtue of effective operation of protective devices specially designed for this system. These devices should be tested periodically since the potential safety hazard from unchecked component failure is high indeed.

## IV - CURRENT STATUS

At the time of this writing (June 1971) the two components of the SMSB facility, the supersonic wind-tunnel and the electromagnetic suspension and balance are at an advanced stage of development as separate entities. All technological problems of a fundamental nature have been solved and thus, although much remains to be done before the prototype facility can be considered operational, it can be safely stated that the feasibility of the concept has been demonstrated. In this last section, the above statement is illustrated with representative results of tests conducted to evaluate the performance of the facility components. The paper concludes with a brief discussion of the remaining tasks.

### (1) Supersonic Wind-Tunnel Tests

Optimization of the internal geometry of the supersonic wind tunnel had two principal goals: first, to increase the tunnel run time as much as possible and second, to decrease the aerodynamic loads on the magnetically suspended model. Both are accomplished simultaneously by maximizing the wind tunnel recovery factor, defined as the ratio of the discharge pressure to the stagnation pressure. A recovery factor of 0.427 was achieved by a successful combination of variable second throat size and length. To this author's knowledge, there is no record of a more efficient Mach-3, axisymmetric wind tunnel in the open literature. Maximum run times of about 5 minutes can be made at low stagnation pressures; this represents a 67% increase over corresponding times for a fixed geometry second throat. At the same time, about 30% decrease in free stream dynamic pressure is made possible by operating the tunnel at these reduced stagnation pressures.

### (2) Magnetic Suspension Tests

Eight tests of the superconducting magnetic suspension system have been conducted to date. Most of these tests were devoted to study performance of individual components and subsystems and develop a satisfactory routine experimental procedure for the system. During this systematic test program, heavy emphasis was placed on probing into the more fundamental aspects of the behavior of key components in an attempt to resolve the basic uncertainties of the overall SMSB concept. For example, initially the performance of the Gradient coils was studied from the point of view of a.c. losses and compatibility with the performance characteristics of the Power Amplifiers, rather than from the point of view of their effectiveness

for producing magnetic field gradients. Safety aspects have also been given high priority for reasons outlined in the previous section.

The fundamental question about the feasibility of using superconductors for magnetic wind-tunnel suspensions has been answered unequivocally in the affirmative. Extensive open-loop testing of gradient coils under conditions far more severe than expected wind-tunnel operating conditions, has shown that coils such as these can be safely driven at the required amplitudes and frequencies with acceptable energy dissipation levels. For specific examples of measurements of a.c. losses of G coils see reference 2.

Two closed-loop tests have been performed using the physical arrangement shown schematically in Figure 8. One Drag Augmentation coil serves the dual function of magnetizing the iron sphere and exerting a bias downward force on it, while the three G-coil pairs and the balancing weights $F_w$ contribute the upward force needed for static equilibrium. Only vertical model position information (x) is fed to the control subsystem for one-dimensional support; a wire "cage" restrains the model from undertaking wide lateral excursions. The level of G-coil support current is varied over a range by simply adding or subtracting weights $F_w$. The response of the control subsystem to perturbation inputs is illustrated in Figure 9, showing oscilloscope traces of a 1 Hz square-wave input signal (top trace) and the corresponding square wave displacement of the model (bottom trace). In this example, a 0.4 V (peak-to-peak) signal resulted in 25 mm displacement. Total increase in helium boil-off rate due to this forced oscillation of the G-coil currents was less than 5 liter/hour.

(3) Remaining Tasks

Clearly, the next step in the development of this facility is to achieve full three-dimensional controlled support of a model. From preliminary attempts made during the last test, it appears that the level of cross-coupling exhibited by the temporary optical position sensor will have to be reduced before reliable three-dimensional support is achieved and the magnetic suspension component of the SMSB prototype facility can be considered operational.

To complete the development of this facility the wind tunnel and the magnetic suspension components must be successfully integrated into a harmonious whole. This will require the construction of a refined model position sensor* compatible with both components and with a model launching and recapturing device which constitutes the interface between the two. Finally, a routine procedure for reliable and efficient operation of the facility, including the acquisition of dynamic stability data will be developed.

## V - ACKNOWLEDGMENTS

As stated in the Introduction, the development of this state-of-the-art facility has been a team effort from the beginning. Many people (faculty, staff, and students, graduate and undergraduate) have contributed with euthusiasm toward the attainment of the objectives of this exciting project. Aside from those specifically refered to in the text, five individuals deserve special recognition: the late Robert Russel, who initiated the development of the power amplifiers, Karl Henderson, who took over that development and carried it to completion; Robert Smoak, who is mostly responsible for the design of the control subsystem; William

* The reader is reminded of a discussion on the model position sensor in section II-4 of this paper.

Towler, who built the model position sensor; and Charles Bankard, whose enthusiasm and dedication to the daily tasks of construction, maintenance and testing of the facility have made a significant contribution to the overall progress level. Though perhaps unusual, it is only fair to acknowledge also the real contributions to all phases of this project made by our NASA contacts, Messrs. H. Wiley, I. Hamlet, and R. Kilgore.

## VI - REFERENCES

(1) Parker, H. M., "Principles, Typical Configurations and Characteristics of the University of Virginia Magnetic Balance" Summary of ARL Symposium on Magnetic Wind Tunnel Model Suspension and Balance Systems Report ARL 66-0135, July 1966. (edited by F. L. Daum).

(2) Moss, F. E., paper C, this symposium proceedings

(3) Jacobson, J. D., et. al., paper K, this symposium proceedings

(4) Parker, H. M, paper S, this symposium proceedings

(5) Bias, J. "Optimization of a Supersonic Wind Tunnel" Masters Thesis. University of Virginia, Department of Aerospace Engr. and Engr. Physics, June 1970.

(6) Parker, H. M., et. al, "Theoretical and Experimental Investigation of a 3-Dimensional Magnetic-Suspension Balance for Dynamic Stability Research in Wind Tunnels", Technical Annual Status Report No. AST-4030-105-68U, Research Laboratories for the Engineering Sciences, University of Virginia, March 1968.

(7) Efferson, K. R., Review of Scientific Instruments, vol. 38, No. 12 pp. 1776-79, December 1967.

(8) Lapins, M., "Optical Date Acquisition System for the Cold Magnetic Balance Wind Tunnel Facility", Masters Thesis. University of Virginia Department of Aerospace Engineering and Engineering Physics, June 1970.

(9) Stephens, T., paper G, this symposium proceedings

TABLE I
Coil Subsystem Characteristics

| | $\tan^{-1}\sqrt{8}$ Coil | DA Coil | MF Coil |
|---|---|---|---|
| Number of coils | 6 | 2 | 1 |
| Dimensions (cm), OD/ID/L | 20/13/1.3 | 51/38/6.4 | 57/55/25 |
| Number of turns | 135 | 3200 | 2800 |
| Type of conductor | GE-150 NbSn tape | 0.076 cm copper clad NbTi | |
| Type of operation | a.c. | d.c. | d.c |
| Room Temp. inductance (H) | 0.004 | 6.2 | 5 |
| Room Temp. Q-factor | 9 | | |
| Max. design current (A) | 350 | 100 | 100 |
| Max. field at suspension point (G) | | 3200 | 6100 |
| Max. gradient at suspension point(G/cm) | 40 | 210 | 0 |

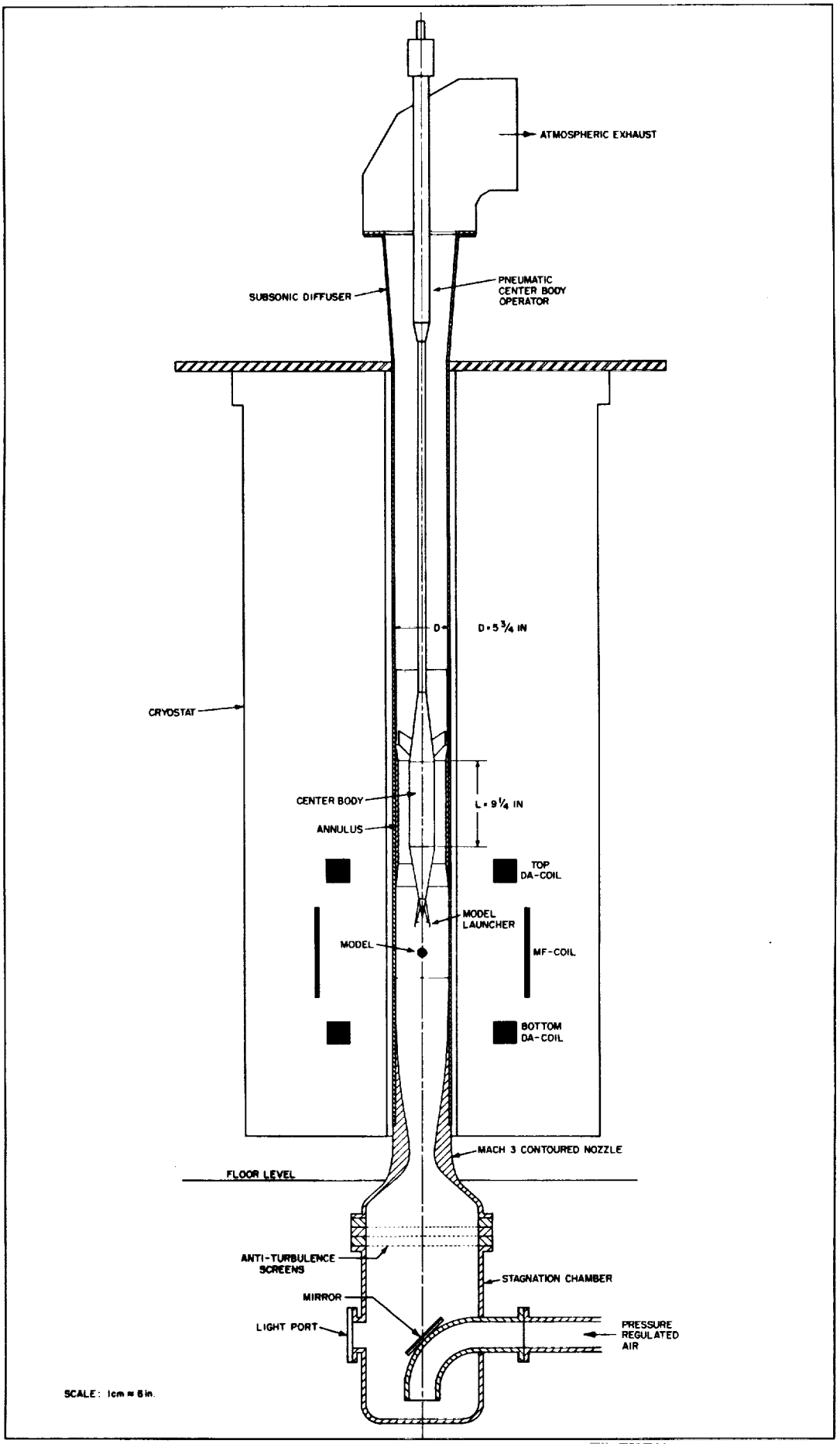


Figure 1. - The Supersonic Wind Tunnel

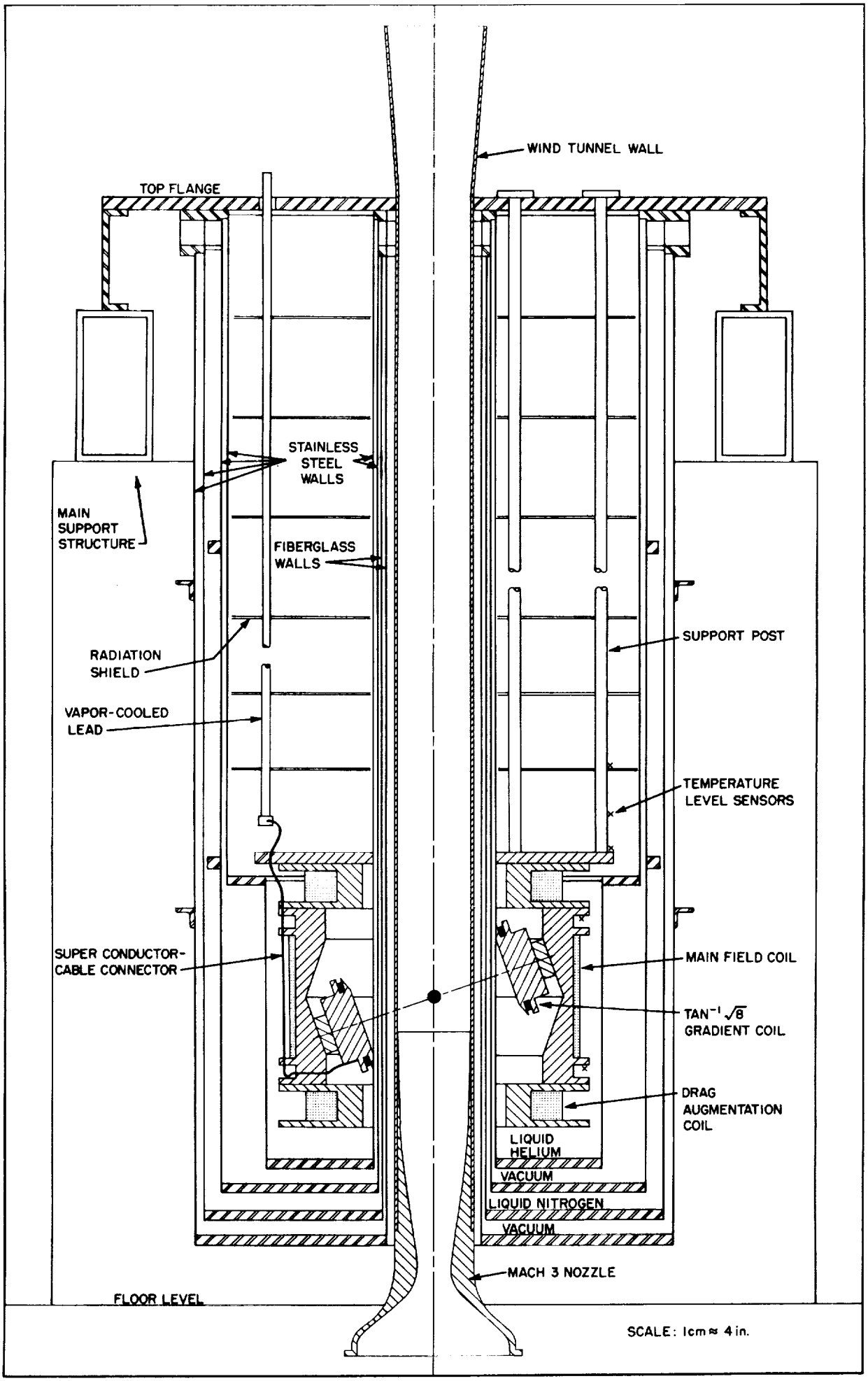


Figure 2. - Coil and Cryogenic Subsystems

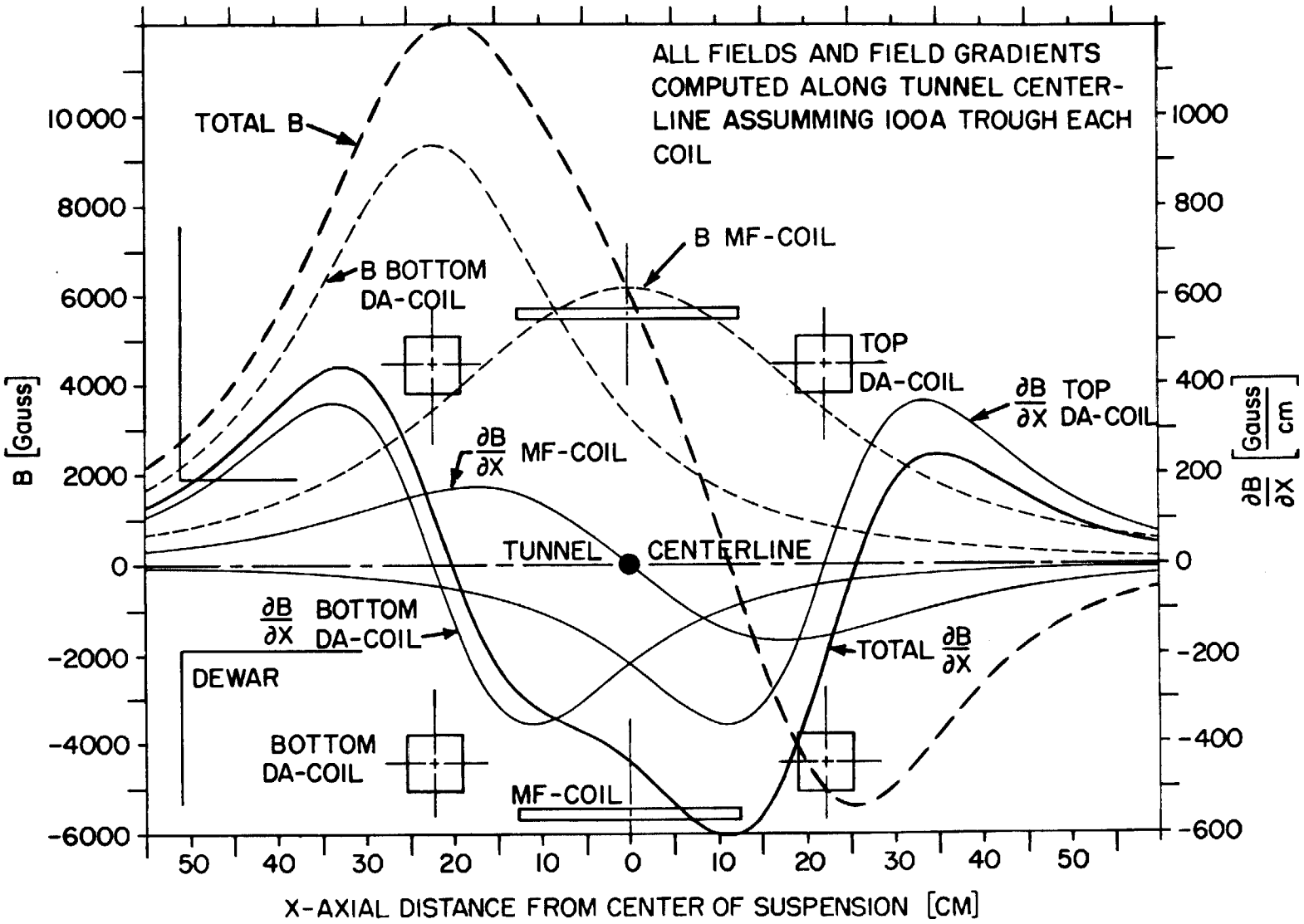


Figure 3. - Axial Magnetic Field and Magnetic Field Gradients Produced by MF and DA Coils

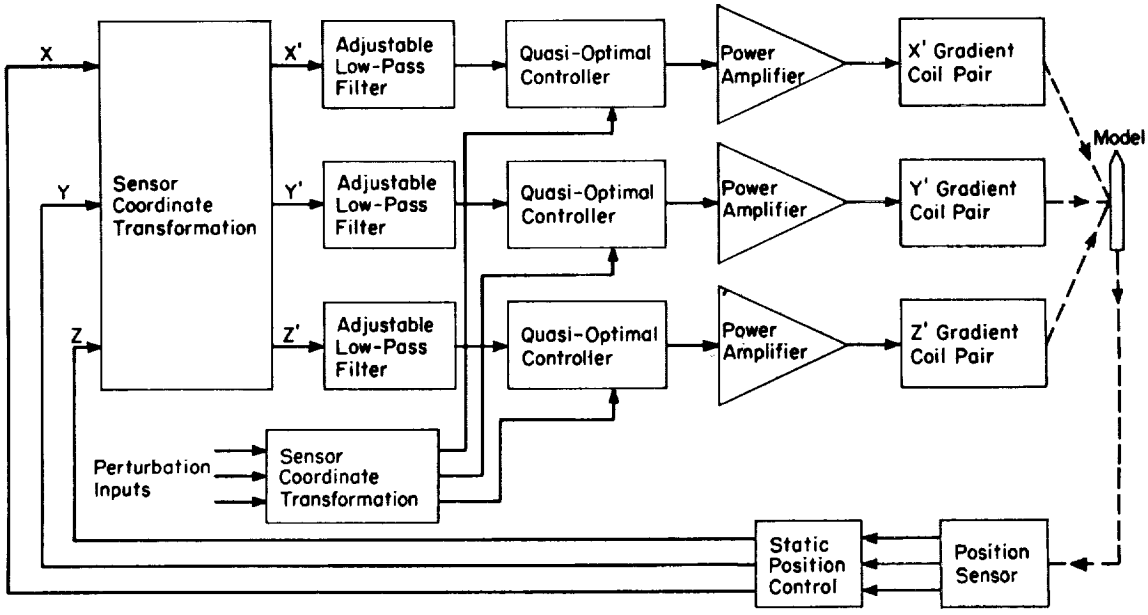


Figure 4. - Functional Block Diagram of Control Loop

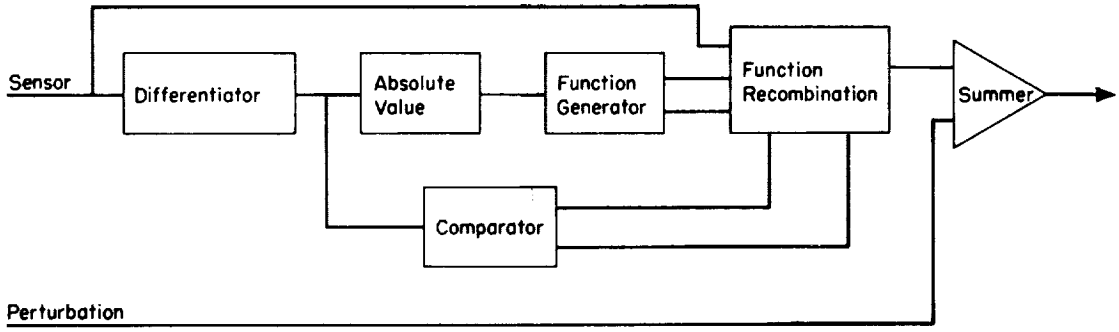


Figure 5. - Functional Block Diagram of Quasi-Optimal Controller

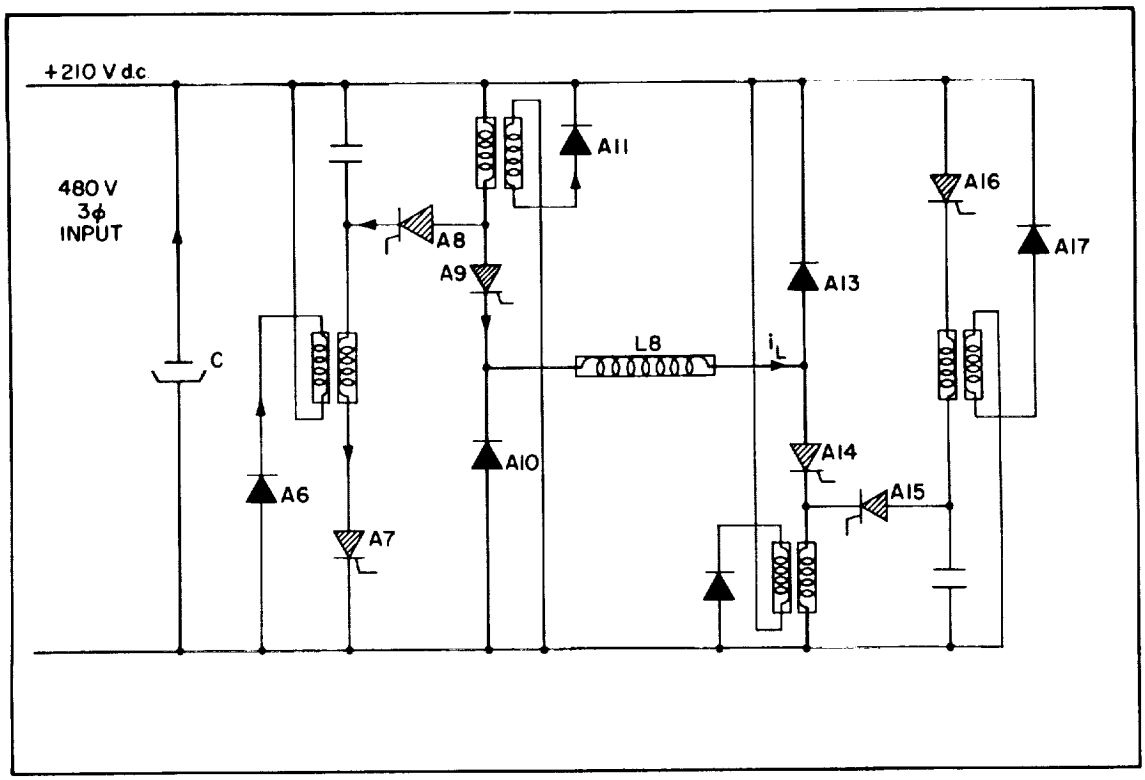


Figure 6. - Simplified Schematic Circuit of Power Amplifier

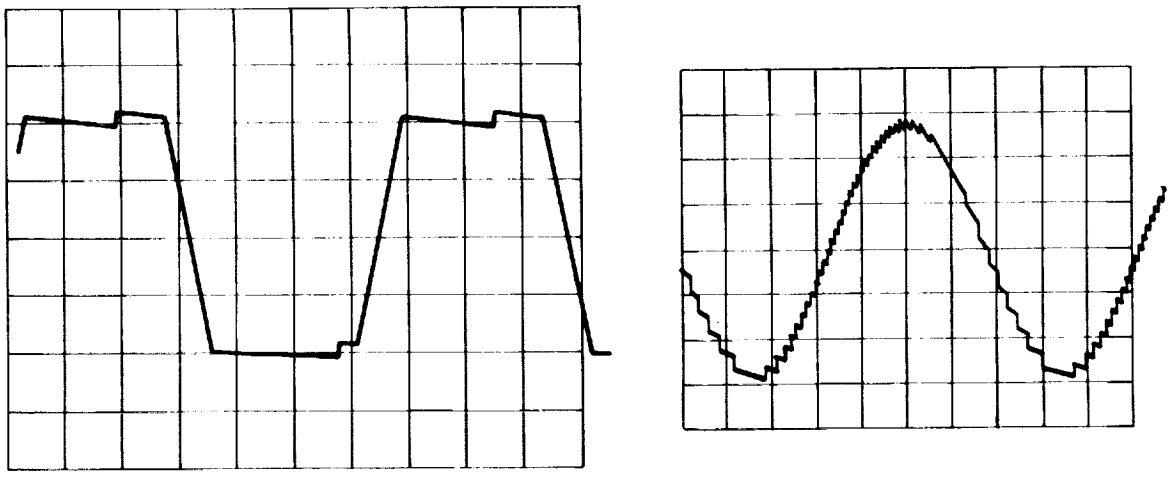

a. Square Wave Response

b. Sign Wave Response

Figure 7. - Current Response to Periodic Inputs

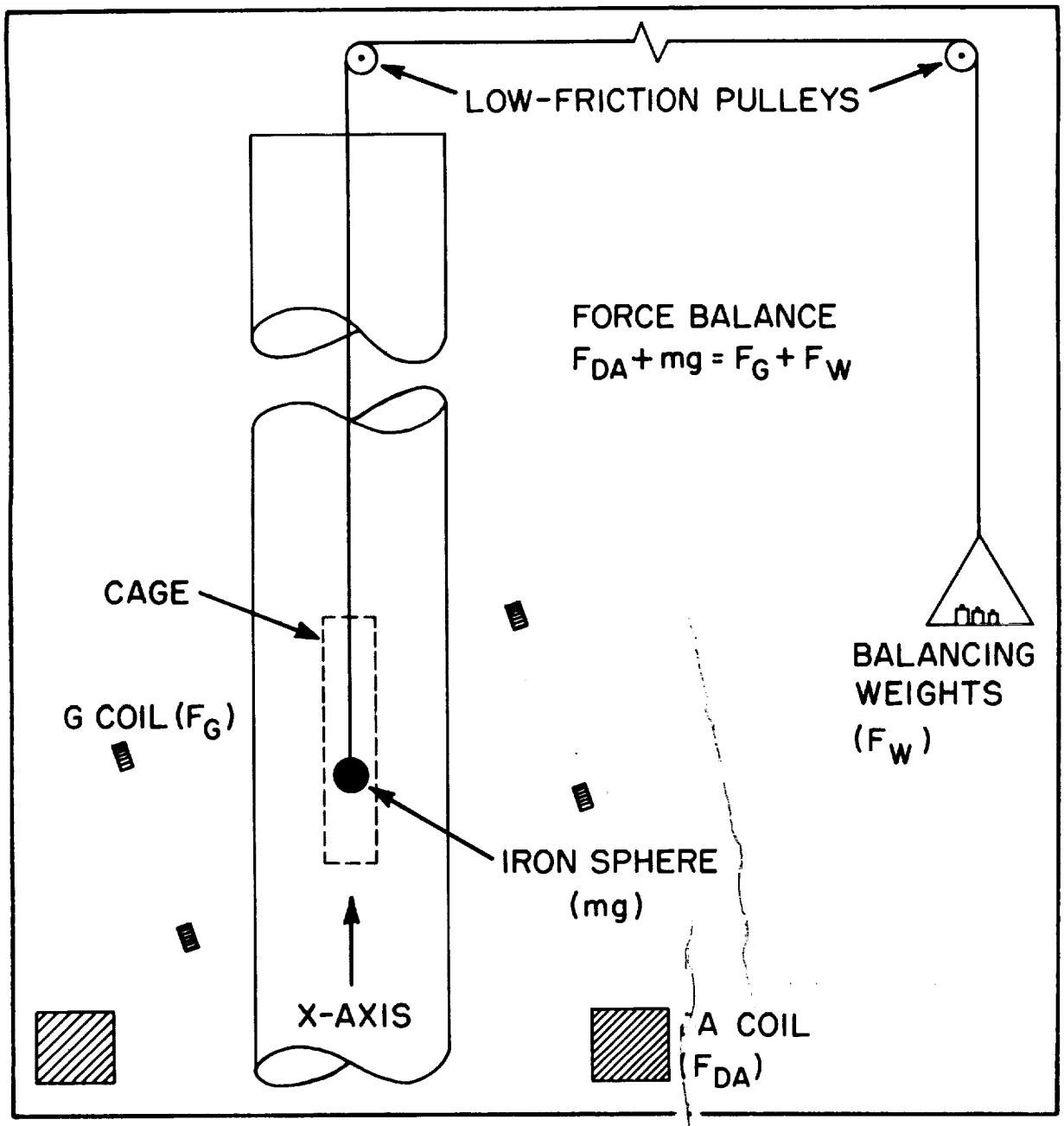


Figure 8. - Sketch of One-Dimensional S port Experiment

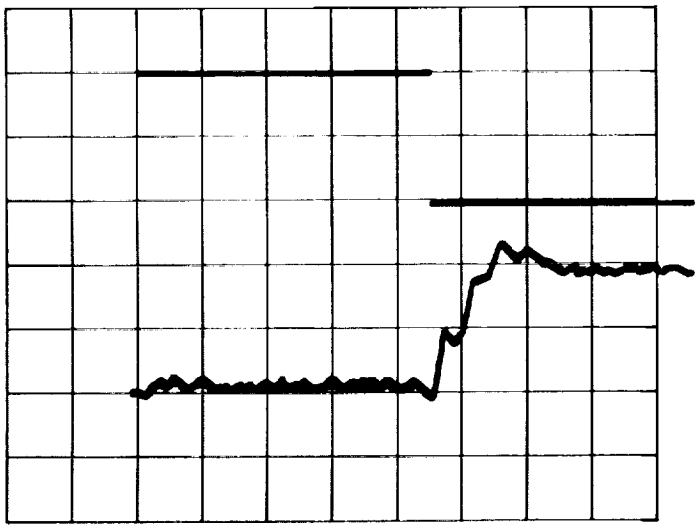

igure 9
Re onse of
Sy em to
Squ e-Wave
Per bation
Inpu

# THE USE OF SUPERCONDUCTIVITY IN MAGNETIC BALANCE DESIGN

by

F. E. Moss*
Department of Aerospace Engineering and Engineering Physics
University of Virginia

## ABSTRACT

The magnetic field and field gradient requirements for magnetic suspension in a Mach 3, 6-in. diameter wind tunnel are stated, along with the power requirements for gradient coil pairs wound of copper operating at room temperature and aluminum cooled to 20°K. The power dissipated is large enough that the use of superconductivity in the coil design becomes an attractive alternative. The problems of stability and A.C. losses are outlined along with the properties of stabilized superconductors. A brief review of a simplified version of the critical state model of C. P. Bean is presented, and the problems involved in calculations of the A.C. losses in superconducting coils are outlined. A summary of A.C. loss data taken at Brookhaven National Laboratories on pancake coils wound of commercially available $Nb_3Sn$ partially stabilized tape is presented and shown as leading to the U.Va. gradient coil design. The actual coil performance is compared with predictions based on the BNL results. Finally, some remarks are presented concerning scaling of the A.C. losses to larger magnetic suspension systems as well as prospects for improved performance using newer multifilament superconductors.

*Present address: Dept. of Physics, University of Missouri, St. Louis, Mo., 63121.

## INTRODUCTION

The support capabilities of magnetic suspension systems are specified in terms of the acceleration, usually measured in units of the acceleration of gravity, which can be imparted to the suspended object; for example, an iron sphere. This is a convenient point of reference since it depends on the field gradient and magnetization and is independent of the size of the supported object (if it is uniformly magnetized). Since, in principle, any supported object could be magnetized to saturation, it is clear that the design of the gradient coils offers the only open-ended possibility for increasing the support capability. Large field gradients, however, require coils which dissipate large amounts of power. The results of an example design[1] for six copper gradient coils operating at room temperature and six aluminum coils operating at 20°K are shown in Figure 1. These coil designs would be suitable for a 10g support system operating on a 6-in. diameter M-3 wind tunnel. While the power dissipated is large in both cases, it is probably manageable and the choice between the two designs would be a question of economic detail. A prime objective of the U.Va. prototype wind tunnel balance program has, however, been to continuously examine the feasibility of scaling the balance design to accommodate larger diameter wind tunnels. A depressing fact is that, for a fixed field gradient, the coil volume, weight, and joulian power all scale as the cube of a linear dimension.[1] The implications of this fact become obvious if we consider operating the aluminum coils at liquid helium temperature (4.2°K) and estimate the cost of refrigeration via the price of liquid helium (~2 to 5 $/ℓ depending on quantity and location of source). Figure 1 shows that the aluminum coils would boil off 406 liters of liquid helium per hour, so that the cost of operating the prototype balance could be as high as about 2000 $/hr.

These considerations lead us to examine the use of superconductivity in the coil design. Certainly, the losses in the prototype balance would be much lower, and hopefully the scaling laws for the superconductors, if they could be discovered, would be more advantageous. In addition, the high current densities possible in superconducting magnets result in more compact coil geometries. Two problems were immediately evident. First, the magnetic suspension of a wind tunnel model is an A.C. problem. Indeed, for a tight enough control loop the gradient coil currents are directly proportional to the aerodynamic forces on the model, which are nonsteady for many cases of interest. While superconducting magnets dissipate zero power in the D.C. mode, it is well known that they are subject to hysteresis-type losses in A.C. operation. Thus an estimate of the magnitude of these losses was necessary in order that sufficient liquid helium refrigerant could be provided to remove the heat generated in the course of a wind tunnel run. The second problem was one of assuring stability against transitions from superconducting to normal states during any phase of the operation. In A.C. operation, certain superconductors "go normal" if the time rate-of-change of field (or coil current) is too great.

In this paper, the physical phenomena responsible for instabilities and A.C. losses in superconductors are reviewed, and a collection of data on tape wound coils is presented. The evolution of the U.Va. gradient coil design is described, and the performance of the final design is compared with projections based on the earlier data and qualitative theoretical considerations. Finally, some preliminary conclusions regarding scaling and possibilities for future improvements resulting from new superconducting wire configurations and materials are put forth.

## THE TRANSIENT BEHAVIOR OF SUPERCONDUCTORS

Postponing, for the moment, the details of why superconductors are subject to A.C. losses, the materials properties shown in Figure 2 clearly delineate the origin of the stability problem. Extremely small thermal and electrical conductivities are characteristic of typical superconducting material compared, for example, with copper. In addition, the only heat sink in a superconductor-copper-liquid helium system is the helium. It is therefore difficult to remove any heat generated in the superconductor, and impossible to store the heat without an unacceptable rise in temperature. Furthermore, if the local temperature at a point in a superconductor exceeds the transition temperature, this "normal spot" tends to propagate throughout the entire material due to the high normal state resistivity. In magnets such an instability frequently drives the entire coil normal resulting in the rapid conversion of the stored energy into heat. Often the coil is destroyed. The numbers on Figure 2 also show how superconducting wire might be "stabilized." At least one dimension must be made very small so that heat generated internally can be transported to the helium bath on small thermal gradient. Thus a conductor might take the form of a thin ribbon or a large number of very fine filaments. When wound into a coil, the conductor must be well ventilated with liquid helium. In addition, should a normal spot develop, it can be stopped from propagating by "shortcircuiting" it with a good conductor. Thus a stabilized superconductor is normally clad with copper. Fully stabilized superconductors have cladding of sufficient cross-sectional area that the entire rated current can be transported in the cladding material alone without exceeding the onset heat current density for film boiling of the liquid helium coolant ($\sim$400 mW/cm$^2$).

The internal losses generated in superconductors stem from changes in the state of magnetization of the superconducting material. Figure 3 shows example magnetization curves for two types of superconducting materials. Type I (soft) materials exhibit perfect diamagnetism until some critical field $H_c$ where superconductivity is destroyed. Since $H_c$ is typically a few hundred gauss, these materials are unsuitable for use in high field magnets. Type II (hard) materials, however, exhibit a state of flux penetration for $H>H_{c_1}$ and are able to maintain a supercurrent until some second critical field, $H_{c_2}$, which

can be a few hundred kilogauss. That the stability of type II superconductors, in the $H>H_{c_1}$ state, was related to internal flux motions was first indicated by a phenomenon called "flux jump instability" observed in magnets wound of unstabilized or partially stabilized superconducting wire. The principle is illustrated in Figure 4(a). Upon uniformly charging a magnet, the internal magnetic field is observed to increase in irregular steps or jumps. On occasion the entire magnet can go normal on a particularly large flux jump, so that it is necessary to charge the magnet very slowly. Once charged, however, the current can be reduced to zero and the magnet subsequently recharged at a much higher rate. This behavior is called training, and results from internally trapped flux remaining from the first charging. Magnetic flux penetrates the superconductors in discrete bundles enclosed in a vortex of supercurrent of quantized circulation.[2] These are called fluxons, each having the value $hc/2e$ ($\simeq 2 \times 10^{-7}$ gauss cm$^2$).[3] As shown in Figure 4(b), each fluxon experiences a Lorentz force in the presence of a transport current. When the Lorentz forces exceed the pinning forces, the fluxons can move through the superconductor generating a voltage as shown by Equation 1. Flux jumping is the result of coherent motions of large numbers of fluxons[4], and training results from trapped flux due to the tendency of the fluxons to become pinned on lattice defects.[5] Equation (2) is the instantaneous power density generated due to flux motion, and shows the dependence on the time-rate-of-change of flux density; thus providing the basis on which flux jump instability is to be understood. In A.C. operation, the loss/cycle can be obtained by integrating the power density over the volume of the superconductor and over one cycle of period T, as shown in Equation (3). This illustrates the hysteretic nature of the losses. In order to evaluate Equation (3) for a given experimental situation, a detailed model accounting for the way in which flux penetrates the sample is required. The first reasonably successful model for the magnetization of high field superconductors was proposed by C. P. Bean[6], based in part on earlier work by K. Mendelssohn.[7] The basic premise is that any electromotive force, however small, will induce a critical current density, $j_c$, which is characteristic of the material, to flow locally. Thus, in view of Equation (1), $j_c$ flows in regions where flux penetrates the superconductor, and further, the flux density decays linearly with distance from the surface in the interior.

Given a surface field, $H_s$, and assuming that $\phi$ = const., it is possible to integrate Equation (3) over the volume of the superconductor. These results are summarized on Figure 5, where two cases of flux penetration in a semi-infinite superconducting slab are shown.[8] For partial penetration, the loss/cycle is proportional to the exposed surface area and the cube of the surface field as shown by Equation (4). An approximate expression applicable to a superconducting ribbon of width W is given by Equation (5). Quite different results follow for complete flux penetration, as shown by Equations (6) and (7). For this condition the loss/cycle is proportional to the volume, the surface field and the thickness, $d_s$, of the

superconductor. Note that the surface field for which flux penetration just becomes complete (the penetration field) depends on the thickness of the superconductor.

The preceding results are ideal in the sense that they apply to an isolated sample of superconductor exposed to a uniform external magnetic field. They are, nevertheless, of value in qualitatively explaining the loss behavior of coils. Figure 6 shows a winding cross section for a pancake coil wound of ribbon of width W. Note that the perpendicular component of the field is shielded from the central turns, so that the entire winding cross section might be regarded in the same way that the single superconducting sample previously was. Thus Equation (8) might be expected to indicate the qualitative behavior for partial flux penetration in both the parallel and perpendicular directions, if the surface fields on the inner and outer turns are not too different, or if some average value is used. Note that this Equation indicates that the losses in coils of various numbers of turns but all wound of tape of the same width should correlate with the average of the perpendicular component of the cube of the field. Equation (9) represents the situation for complete penetration, though this condition can rarely be achieved in pancake coils of more than a few turns, since the outer turns tend to go normal before the central turns suffer penetration.

The Bean model thus predicts that for superconducting coils in general the losses should go linearly with frequency (constant loss/cycle) and with the cube of the magnetic field. In addition, for ribbon wound pancake coils a correlation with the perpendicular field component is to be expected. As shown in an excellent review by Wipf[9], these predictions are verified for a surprisingly wide variety of superconducting materials and coil geometries.

## SOME EXPERIMENTAL DATA AND THE U.VA. GRADIENT COIL DESIGN

The current gradient coil design for the U.Va. balance consists of 135 turns of partially stabilized $Nb_3Sn$ tape wound in a 5-in. I.D. by 7-in. O.D. by 1/2-in. wide pancake. The tape is General Electric type 150. This is actually a second-generation coil design. The original design called for fully stabilized NbTi, 7 strand cable manufactured by Atomics International. Though stability was not expected to be a problem, this design was abandoned because of a fear that the losses would be intolerably high due to the large quantity of superconducting material comprising the cable. This in fact proved to be the case. Measurements, to be described in the following paper by I. L. Hamlet and R. S. Kilgore, on a cable-wound gradient coil indicated losses of about one order-of-magnitude greater than an equivalent tape-wound coil. The losses to be expected from the tape-wound coil were estimated from data obtained at Brookhaven National Laboratories.[10] Some of these data for single pancake coils are shown on Figure 7, where the loss/cycle meter is plotted against the average of

the square of the perpendicular field component. The operating point for the U.Va. gradient coil is shown on the horizontal scale, and a range of expected losses to be expected for a gradient coil pair is shown on the vertical scale expressed in terms of the liquid helium boil-off rate. Even the upper limit of this range is an acceptable boil-off rate in view of the liquid helium storage capacity of the wind tunnel balance dewar.[11] On Figure 8, some additional loss data for tape-wound, pancake coils is shown. These data were taken at the Langley Research Center and are described more completely in the following paper. Figure 8 once again demonstrates the linear relation between the loss/cycle and the cube of the field, where NIG is the ampere turns times a geometric factor representing the effectiveness of each coil design for producing a field gradient at the nominal support point. The measured gradient coil performance is shown on Figure 9, and compares favorably with predictions based on the BNL data of Figure 7. Since the current excursion from zero to 350A in 16 millisec represents the maximum capability of the power amplifiers, the stability of the coils is demonstrated under conditions of maximum time rate-of-change of field.

## SCALING

It has been shown that for constant aerodynamic forces on the model, and assuming the same Mach number and dynamic pressure for the wind tunnels, the gradient field requirements scale inversely as a characteristic length[12], and that this leads to the linear scaling law for gradient coil ampere turns.[13] The loss/cycle for superconducting gradient coils would thus scale as the cube of a linear dimension for partial penetration and directly with a linear dimension for complete penetration. These results are summarized on Figure 10. It should be noted, however, that Parker[12] has presented an argument which suggests that a characteristic frequency for a magnetic balance system scales inversely with linear dimension. If this is indeed the case, the losses for superconducting gradient coils should scale as the square of a linear dimension for partial penetration, while for complete penetration the losses do not scale! In any case, it is clear that operation in the region of complete flux penetration results in a more desirable scaling law, while it has already been noted that complete penetration is unlikely for tape-wound coils.

## FUTURE POSSIBILITIES

The problem is to find a conductor configuration which admits complete flux penetration at a relatively low field. Smith, et. al.[14], have recently suggested the use of twisted multifilamentary conductors as a means of lowering the penetration field. This conductor consists of many extremely fine filaments of superconductor imbedded in a copper matrix and twisted at a certain pitch determined by the operating frequency of the coil. The filaments are thus inductive and

result in an electric field directed along the conductor axis when the transport current is time varying. Since each and every filament is exposed to the electric field, the critical state model supposes that $j_c$ flows in a flux penetration region on each filament even for low fields. Stated in a different way, no central turns in a coil are shielded from the magnetic field as is the case in tape-wound coils and coils wound of untwisted material, nor are the individual filaments shielded from each other. In order to achieve complete penetration, the field must penetrate superconducting material only to a depth equal to the radius of an individual filament. The transition from partial to complete penetration can be expected to occur at low fields for small diameter filaments. These assertions have been strikingly verified in experiments by Dahl, et. al.[15] as shown by the data on Figure 11. Here two coils were wound of the same multifilament conductor consisting of 81 cores of ≃.0014-in. diameter each. In one case the multifilament was twisted while for the other it was not. The results strikingly demonstrate the advantages of twisting, at least in the high field region, and show the transition from partial flux penetration (slope = 3) to complete penetration (slope = 1) as occurring somewhere around 4 kilogauss.

In conclusion, it is possible to state that the multifilament superconductors hold great promise for significant improvements in scaling the gradient coil losses. In the most optimistic case, they suggest that these losses do not scale.

## REFERENCES


1. H. M. Parker, G. B. Matthews, and A. R. Kuhlthau, "A Prototype Magnetic Windtunnel Balance," Report No. AEEP-NASA-235-66U, June 1966.

2. A. A. Abrikosov, Soviet Phys. JETP 5, 1174 (1957).

3. B. S. Deaver and W. M. Fairbank, Phys. Rev. Letters 7, 43 (1961).

4. M. R. Wertheimer and J. de G. Filchrist, J. Phys. Chem. Soc. 28, 2509 (1967).

5. S. L. Wopf, Phys. Rev. 161, 404 (1967).

6. C. P. Bean, Phys. Rev. Letters 8, 250 (1962); and Rev. Mod. Phys. 36, 31 (1964).

7. K. Mendelssohn, Proc. Roy. Soc. (London) A152, 34 (1935).

8. F. DiSalvo, Avco Everett Res. Lab., Rept. AMP-206 (1966).

9. S. L. Wipf, Proc. 1968 Summer Study of Superconducting Devices and Accelerators, BNL 50155 (C-55) (1968), p. 511.

10. G. H. Morgan, P. F. Dahl, W. B. Sampson, and R. B. Britton, BNL Rept. 12586R, and J. Appl. Phys. 40, 1821 (1969).

11. Described in paper A by R. N. Zapata.

12. H. M. Parker, R. N. Zapata, and G. B. Matthews, U.Va. Rept. No. AST-4030-105-68U, 1968.

13. H. P. Wilkinson, Jr., "Scaling A.C. Superconducting Coils for Windtunnel Balance Applications," U.Va. School of Engineering and Applied Science, Senior Thesis (1971).

14. P. F. Smith, M. N. Wilson, C. R. Walters, and J. D. Lewin, Proc. 1968 Brookhaven Summer Study on Superconducting Devices and Accelerators, BNL 50155 (C-55) (1968).

15. P. F. Dahl, G. H. Morgan, and W. B. Sampson, J. Appl. Phys. 40, 2083 (1969).

MAGNETIC REQUIREMENTS FOR 1g SUPPORT CAPABILITY ON AN IRON SPHERE ARE:

- ~ 5 KILOGAUSS MAIN FIELD, AND
- ~100 GAUSS/CM GRADIENT FIELD

AT THE SUPPORT POINT.

FOR THE 6" DIAMETER WIND TUNNEL, THE POWERS DEVELOPED IN A GRADIENT COIL SET ARE:

- ~320 KILOWATTS FOR ROOM TEMPERATURE COPPER ($\rho$ = 2$\mu\Omega$ CM)
- ~270 WATTS (406 $\ell$LHe/HR) FOR 20°K ALUMINUM ($\rho = 1.7 \times 10^{-3} \mu\Omega$ CM)

FIGURE 1

| | TYPICAL SUPERCONDUCTING MATERIAL | COPPER | LIQUID HELIUM AT 4.2°K |
|---|---|---|---|
| THERMAL CONDUCTIVITY (mw/CM °K) | 0.4 - 1.2 | 70000 | 2.72 |
| SPECIFIC HEAT (mJ/GM °K) | ~0.2 | 0.1 | 4480 |
| NORMAL STATE RESISTIVITY $\mu\Omega$•CM | 25 - 30 | 0.03 | ---- |

REMARKS:

1. THERMAL AND ELECTRICAL CONDUCTIVITY OF COPPER ARE MANY ORDERS OF MAGNITUDE LARGER THAN THE SUPERCONDUCTORS.
2. THE ONLY SIGNIFICANT HEAT SINK IS THE HELIUM.
3. THEREFORE, FOR STABILITY, SUPERCONDUCTORS MUST BE OF SMALL DIMENSION, ENCASED WITH COPPER, AND WELL VENTILATED IN A LARGE BATH OF HELIUM.

FIGURE 2

PROPERTIES AFFECTING THE STABILITY OF SUPERCONDUCTORS

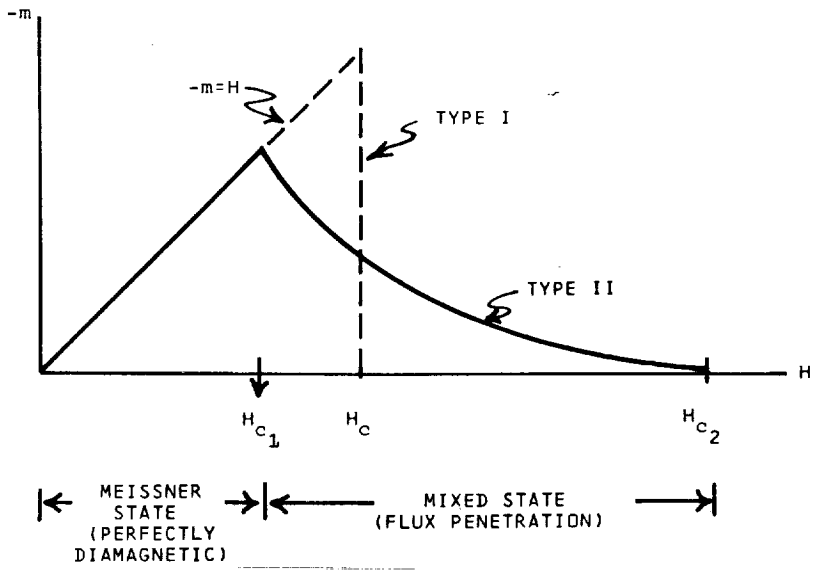


FIGURE 3

TYPE II SUPERCONDUCTORS CHARACTERIZED BY THREE MATERIALS DEPENDENT PARAMETERS: $H_{c_1}$, $H_{c_2}$ AND $j_c$

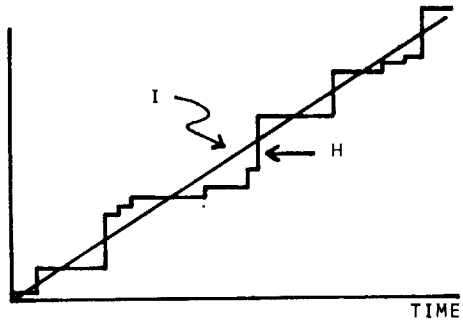


(A) FLUX JUMPING FOR $H > H_{c_1}$

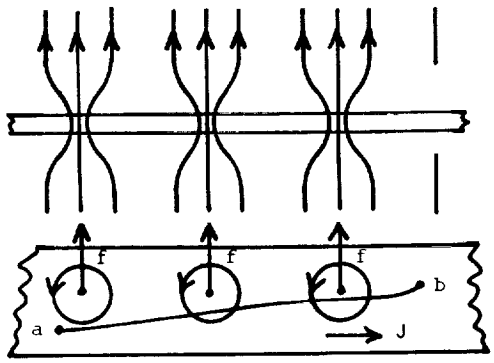


(B) FLUX PENETRATION FOR $H > H_{c_1}$

$$\int_a^b E \cdot d\ell = \dot{\Phi}_{ab} = V_{ab} \qquad (1)$$

INSTANTANEOUS POWER DISSIPATED PER UNIT VOLUME

$$dP = d(EJ) = d(\dot{\phi}J) \qquad (2)$$

IN THE A.C. MODE:

$$\text{LOSS/CYCLE} = \int_{vol} \int_t^{t+T} dP \qquad (3)$$

FIGURE 4

CHARGING A SUPERCONDUCTING COIL WITH A CONSTANT CURRENT SOURCE

ASSUMPTIONS: $\dot{\phi}$ = CONST

$j$ = CONST = $j_c$ IN FLUX PENETRATION REGION

$j$ = 0 ELSEWHERE

THUS: $\frac{dB}{dx} = 4\pi j_c$

(A) PARTIAL FLUX PENETRATION

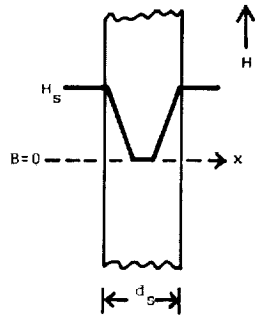


LOSS/CYCLE • UNIT SURFACE AREA

$$\approx \frac{2}{3}\frac{\mu_o H_s^3}{j_c} \quad (4)$$

LOSS/CYCLE • UNIT LENGTH

$$\approx \frac{4}{3}\frac{\mu_o H_s^3}{j_c} w \quad (5)$$

(B) COMPLETE FLUX PENETRATION

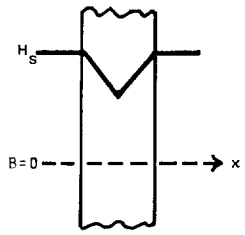


LOSS/CYCLE • UNIT VOLUME

$$= \mu_o j_c H_s d_s \quad (6)$$

LOSS/CYCLE • UNIT LENGTH

$$\approx \mu_o j_c H_s d_s^2 w \quad (7)$$

FIGURE 5

BEAN'S CRITICAL STATE MODEL

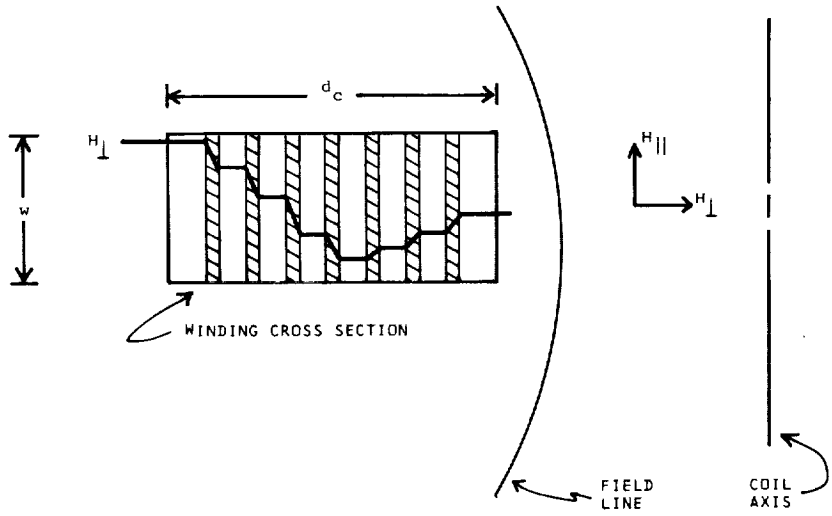


(A) FOR PARTIAL PENETRATION IN BOTH DIRECTIONS:

$$\frac{\text{LOSS/CYCLE}}{\text{AVE. WINDING CIRCUMFERENCE}} \approx \frac{4}{3}\frac{\mu_o}{j_c}\left[H_{s\perp}^3 dc + H_{s\parallel}^3 w\right] \quad (8)$$

(B) FOR COMPLETE PENETRATION IN BOTH DIRECTIONS:

$$\frac{\text{LOSS/CYCLE}}{\text{AVE. WINDING CIRCUMFERENCE}} \approx \mu_o j_c \left[H_{s\perp} d_c^2 w + H_{s\parallel} w^2 d_c\right] \quad (9)$$

FIGURE 6

SHIELDING EFFECT IN PANCAKE COILS

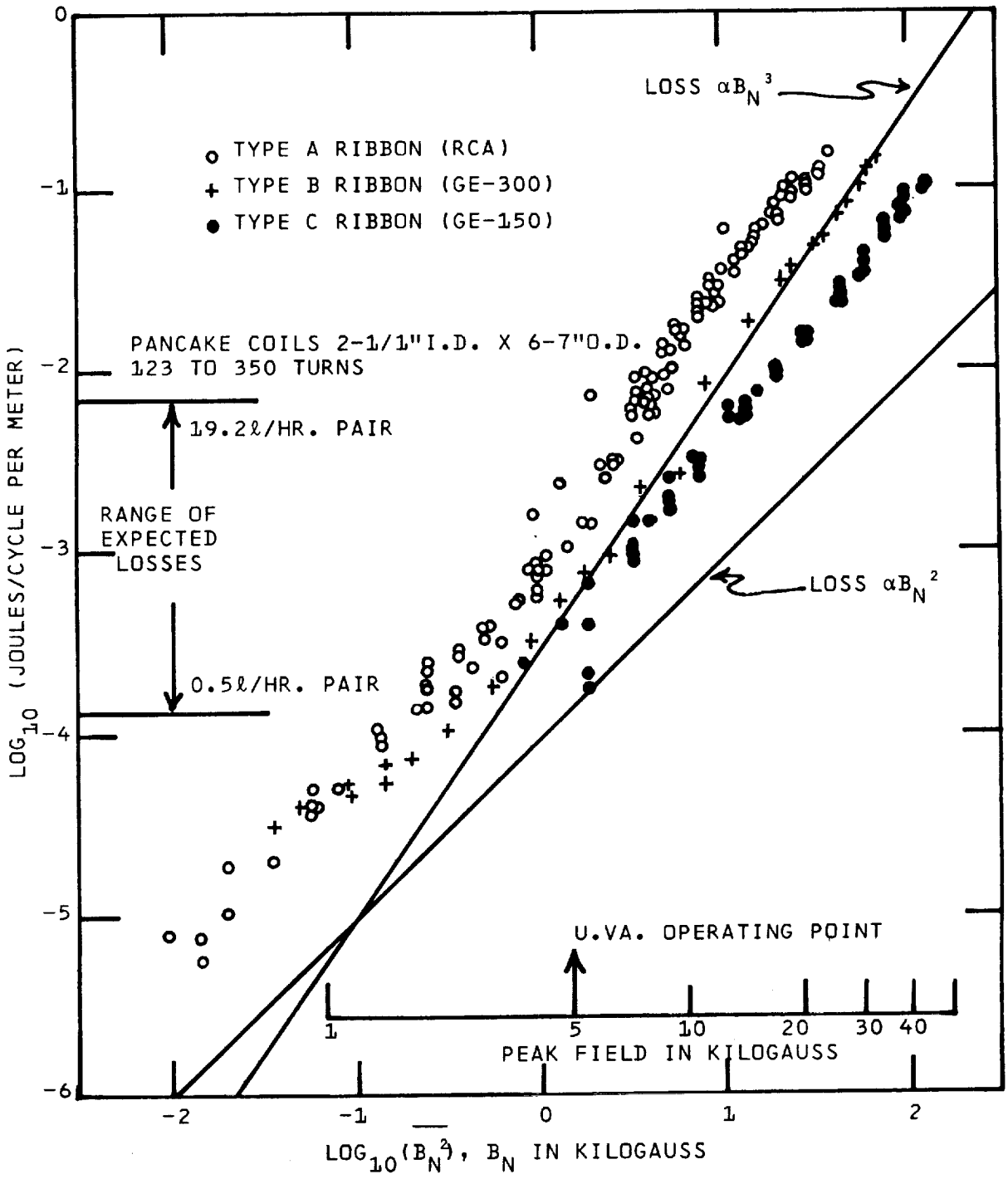


(AFTER MORGAN, DAHL, SAMPSON & BRITTON-BNL 12586R)

FIGURE 7

SUMMARY OF BROOKHAVEN DATA FOR TAPE-WOUND COILS

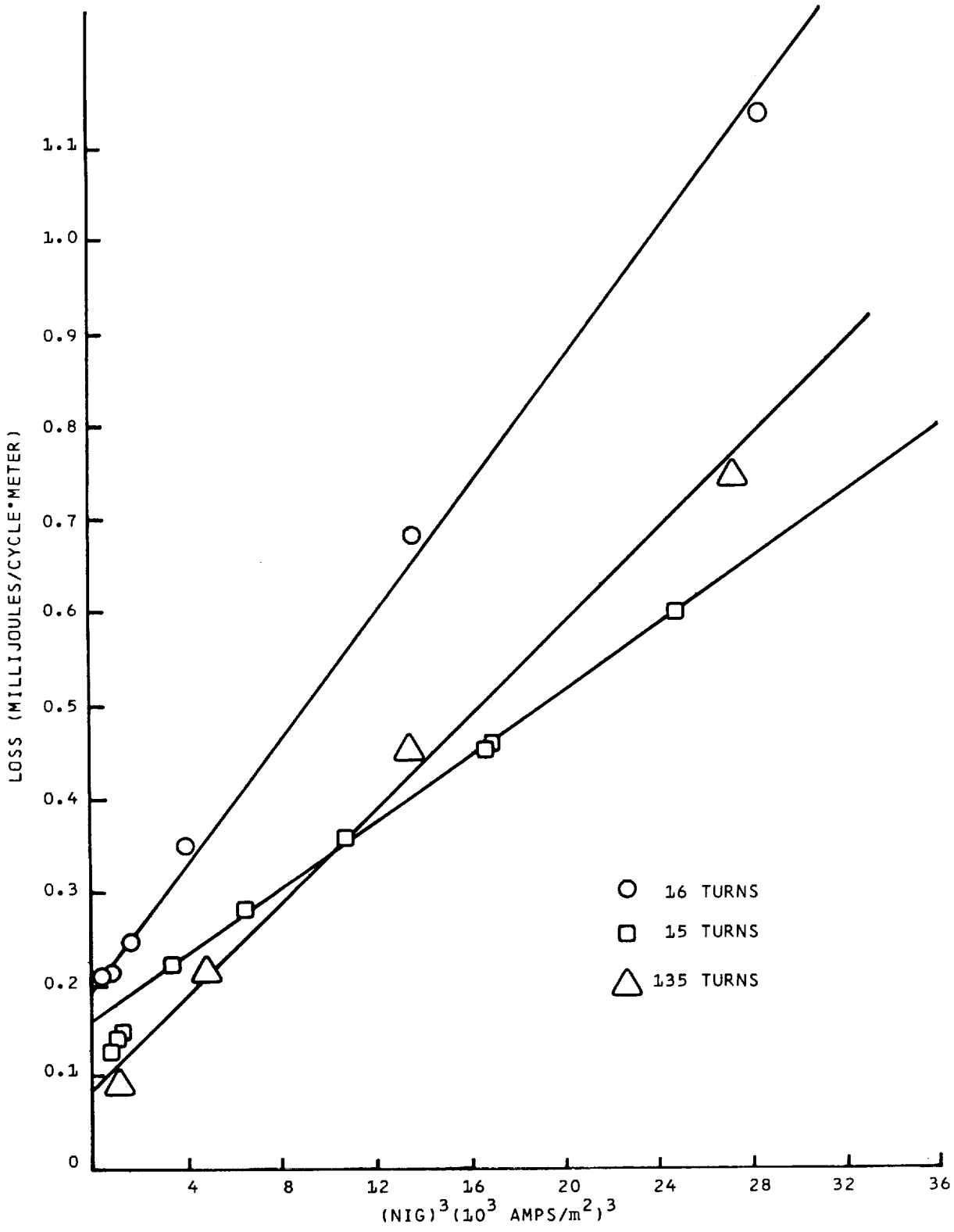


FIGURE 8

LOSSES IN U.VA. TAPE-WOUND COILS

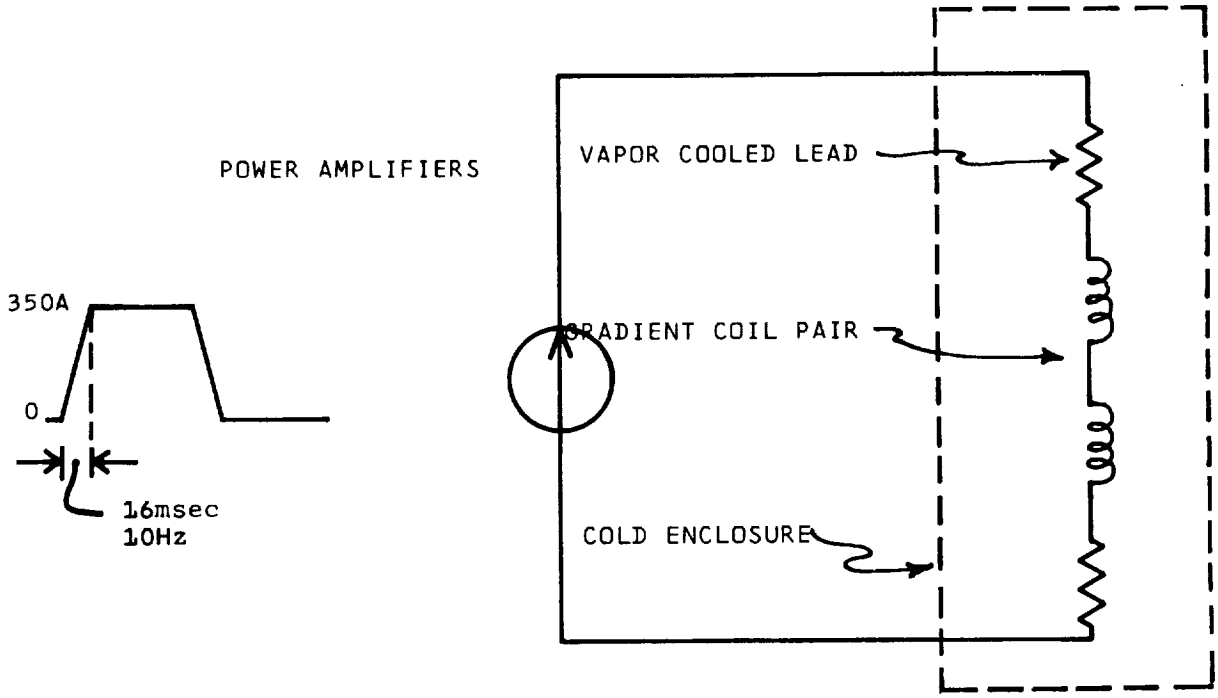


| | | |
|---|---|---|
| TOTAL BOIL OFF | 16 TO 20 ℓ/HR | |
| -EST. LEAD LOSSES | -4 | -4 |
| EST. COIL LOSSES | 12 | 16 |

SINGLE COIL SPECS: 135 TURNS G.E. 150 TAPE
5 IN. I.D. X 7 IN. O.D.
4 mh

FIGURE 9
GRADIENT COIL PERFORMANCE

IN ORDER TO BALANCE THE AERODYNAMIC FORCES:

$$\frac{\nabla B_1}{\nabla B_2} = \frac{L_2}{L_1} \simeq \frac{N_2 I_2}{N_1 I_1}$$

(A) PARTIAL FLUX PENETRATION

$$\frac{P_2}{P_1} \simeq \left(\frac{N_2 I_2}{N_1 I_1}\right)^3$$

(B) COMPLETE FLUX PENETRATION

$$\frac{P_2}{P_1} \simeq \frac{N_2 I_2}{N_1 I_1}$$

FIGURE 10
SUMMARY OF SCALING LAWS FOR WIND TUNNEL BALANCES
USING SUPERCONDUCTING COILS

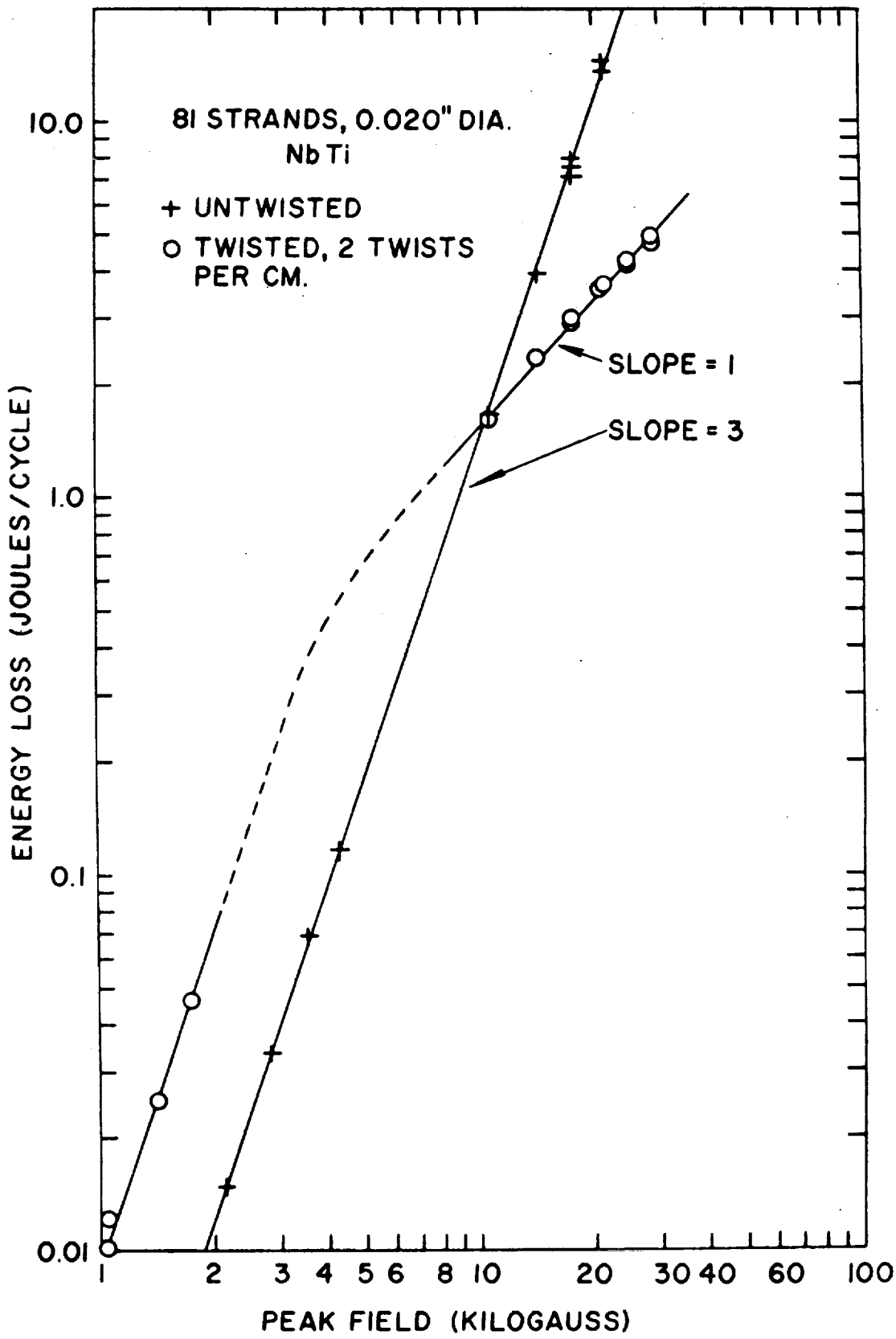


FIGURE 11

EFFECT OF TWISTING ON MULTIFILAMENT
(AFTER: DAHL, MORGAN, SAMPSON)

# DATA ACQUISITION AND REDUCTION FOR THE UVA SUPERCONDUCTING MAGNETIC SUSPENSION AND BALANCE FACILITY[†]

by

I.D. Jacobson,[††] J.L. Junkins,[††] and J. R. Jancaitis[†††]
Department of Aerospace Engineering and Engineering Physics
University of Virginia

## ABSTRACT

The problems associated with data acquisition and reduction in the U.Va. superconducting magnetic suspension and balance facility are similar to those in free-flight ranges (or tunnels). The model undergoes a "Quasi-six-degree-of-freedom" motion which must be monitored both in position and angular orientation from which the aerodynamics must be inferred. The data acquisition problem is made more difficult because geometric constraints prevent direct visual access to the model in the Mach 3 wind tunnel. The methods, accuracies and problems associated with the acquisition of data are discussed.

[†]This work was supported under NASA Grants 47-005-029, 149, 112

[††]Assistant Professor of Aerospace Engineering

[†††]Research Specialist

## 1.0 Introduction

The problems associated with data reduction in the U.Va. superconducting magnetic suspension and balance facility (SMSB) are similar to those in free-flight ranges (or tunnels). A complete description of this facility can be found in reference 1. The model undergoes a "quasi-six-degree-of freedom" motion which must be monitored in both position and angular orientation, from which the aerodynamics must be inferred. The advantages of this facility over a conventional free flight facility is the ability to test over "long" times and gather more data, making the determination of model aerodynamics more accurate. In addition the increased length of time enables the transient part of the motion to decay allowing observation and analysis of steady-state motion. This promises to be a useful technique, as will be described below.

The precision with which we can determine the aerodynamics depends on two factors: first, the accuracy of the data acquisition technique used; and, second, the manner in which the errors propagate through the mathematical motion model and data reduction techniques. Here we will primarily be concerned with the latter; however, since it is an integral part of the data reduction scheme we will first discuss the data acquisition problem.

## 2.0 Data Acquisition

There are three methods for data acquisition in the U.Va. magnetic suspension facility. These are shown in Figures 1, 2, and 3. The first of these-the optical sensor (Figure 1), used to provide feedback for the control system, will also provide the primary data source for the data reduction process. The optical system is a conventional light beam-photocell system designed and calibrated to give position and angular data. The model geometry is one of the optical sensor design criteria, and hence, changing model geometry may require a new optical sensor design and calibration.

The optical system will hopefully be replaced by an electromagnetic sensor of the MIT type (Figure 2) which at this time is still under development. The main problems with the electromagnetic system arise from its use near a high alternating current source. The electromagnetic sensor will require less area in the annulus around the tunnel and thus allow a larger diameter test section. The primary motivation for development of the electromagnetic sensor is its invariance to model changes.[2]

The fiber optic system[3] (Figure 3) was designed primarily for use as a visual cue for the operator, who, due to the helium dewar, does not have a direct line of sight to the model. The distortion created (mostly barrel type), shown in Figure 4 can be compensated for by an extensive calibration procedure. This source of data is difficult to incorporate into the data reduction process since it requires a relatively large preprocessing effort and its estimated accuracy is an order of magnitude less than the other two systems as is illustrated in Table I.

Table I
Data Acquisition Systems Accuracies (estimates)

| Sensor Type | Position | Angles |
|---|---|---|
| Optical | .1 mm (3 axes) | .05 degrees (2 planes) |
| Electromagnetic | .1 mm (3 axes) | .01 degrees (2 planes) |
| Fiber Optic | 1 mm (3 axes) | .1 degree (1 plane) |

## 3.0 Control Technique

In order to understand the concepts of data reduction as applied to

the model motion in the U.Va. magnetic suspension facility it is first necessary to understand the "quasi-six-degree-of-freedom" nature of the motion. By "quasi-six-degree-of-freedom" we mean the model is free to both rotate and translate at frequencies above some cutoff imposed by the SMSB control system. The feedback controller is designed to control only low frequency (O(10 hz)) and DC components of the model motion leaving the high frequency motion "untouched".

The maximum excursion of the model from the tunnel centerline at high frequencies given by

$$d_{max} = \frac{\alpha_{max} I_z}{m\ell} \qquad (3.0\text{-}1)$$

where $\alpha_{max}$ is the maximum angle of attack, $I_z$ the pitch moment of inertia, m, the mass, and $\ell$ the distance between center of pressure and center of gravity.

For a typical model with a natural aerodynamic frequency of 35 hz the maximum displacement can be kept within 1 cm of the centerline.

In principle a controller which will leave the model aerodynamics "untouched" (i.e. not affect the roots of the characteristic equation associated with the aerodynamics) can be designed. It is one that requires feedback in position, velocity, angle and angular rate, the gains of each being determined by the method of Bass and Gura.[4] This method requires the knowledge of the aerodynamic properties of the model a priori, and freedom to use feedback in all the problem variables. Although feasible, this method is less desirable than a simple position-velocity controller.

An analysis of a simple position-velocity controller with a 3 hz natural frequency and $\sqrt{2}$ damping ratio has been carried out based on rather crude estimates of model aerodynamics. The indications are that there is little, if any, interaction with the model motion due to aerodynamics.

Two sources of error were examined:

1. Errors due to uncertainties in model aerodynamics.
2. Errors due to uncertainties in the position of the magnetic center with respect to the center of mass.

As can be seen from Figure 5 there is an insignificant effect on the damped natural frequency of the model and a small effect (about 2%) on the damping exponent. The error introduced by the controller into the damping exponent can easily be calibrated with wind off and used to compensate the later results of the inversion process to obtain aerodynamics. For the steady-state case a frequency response analysis for a typical model with and without controller was conducted. The results are given in Table II.

Table II

Frequency Response Analysis

| Driving Frequency (Rad/Sec) | $\lvert\Delta/M_{ext}\rvert$ (Rad/Ft-lb) | | $\lvert X/M_{ext}\rvert$ (Cm/Ft-lb) | |
|---|---|---|---|---|
| | Free | Controlled | Free | Controlled |
| 150 | 1.56036 | 1.56981 | 17.4107 | 17.5269 |
| 175 | 1.91601 | 1.92581 | 15.7085 | 15.7964 |
| 200 | 2.45552 | 2.46566 | 15.4143 | 15.4838 |
| 225 | 2.96322 | 2.96845 | 14.698 | 14.7285 |
| 250 | 2.65051 | 2.64787 | 10.6494 | 10.6414 |
| 275 | 1.88953 | 1.88687 | 6.27438 | 6.26686 |
| 300 | 1.33748 | 1.33608 | 3.73196 | 3.7287 |

The conclusions to be drawn from the effects of the controller on the characteristic equation and the frequency response of the model are as follows:

1. For transient analyses the damping exponent may be affect by some small percentage (about 2-5%). This can be compensated for a posteriori.
2. There is insignificant effect on the frequency.
3. The forced steady-state motion is essentially unaffected by the controller.

Thus for the analysis of aerodynamics discussed in the next sections the model will be considered to be in free-flight with no inputs due to the feedback control system. This, it is felt, is the unique feature of this wind tunnel system - "long term" free-flight data.

## 4.0 Mathematical Models

4.0.1 The first mathematical model to be considered is well known linearized equations for a rolling missile with trigonal or greater symmetry[5]

$$[2\mu D - C_{z_\alpha} - C_{z_{\dot\alpha}} D - i\hat{p}_o(C_{z_{p\beta}} + C_{z_{p\dot\beta}} D)]A - [2\mu + C_{z_q} - i\hat{p}_o C_{z_{pr}}]D\Delta = F_{ext} \quad (4.0.1\text{-}1)$$

$$-[C_{m_\alpha} + C_{m_{\dot\alpha}} D + i\hat{p}_o(C_{m_{p\dot\beta}} D)]A + [i_B D^2 - C_{m_q} - i\hat{p}_o(i_A - C_{m_{pr}})]D\Delta = M_{ext} \quad (4.0.1\text{-}2)$$

where the C's are the aerodynamic coefficients, $\mu$ the nondimensional mass, $i_A$ and $i_B$ nondimensional inertias, $\hat{p}_o$ the nondimensional roll rate, D the derivative operator, A the complex angle of attack, $\Delta$ the complex orientation angle, $F_{ext}$ and $M_{ext}$ external driving functions. These equations have the familiar quadricyclic solution for either of the variables A or $\Delta$, e.g.

$$\Delta = K_1 e^{(\lambda_1 + i\omega_1)t} + K_2 e^{(\lambda_2 + i\omega_2)t} + K_3 e^{i\omega_3 t} + K_4 \quad (4.0.1\text{-}3)$$

where $K_i$ is the initial amplitude of the mode, $\lambda_i$ is the damping rate of the mode, $\omega_i$ is the frequency of the mode, and $\phi_i$ is the phase angle of the mode. The subscripts 1, 2, 3, and 4 refer to the precession, nutation, rolling trim, and nonrolling trim modes respectively.

The constants $K_i$, $\lambda_i$, $\omega_i$, and $\phi_i$ contain the information needed to obtain the aerodynamic coefficients. The precision to which the coefficients can be determined depends on the precision to which the data is known; examples of this will be given below.

Equation 4.0.1-3 contains the information needed to fit both transient (all four modes of motion) and steady-state (just the $K_3$ and $K_4$ modes of motion) data. The inversion process for transient case yields the aerodynamics in one run using the following relationships

$$C_{m_\alpha} = (\omega_1\omega_2 - \lambda_1\lambda_2)2I_y/\rho U^2 Sd \quad (4.0.1\text{-}4)$$

$$C_{mq} + C_{m_{\dot\alpha}} = [(\lambda_1 + \lambda_2) + \frac{\rho US}{2m}(-C_{z_\alpha} - C_D)]4I_y/\rho USd^2 \quad (4.0.1\text{-}5)$$

$$C_{m_{p\beta}} = [\frac{\omega_1\lambda_2 + \omega_2\lambda_1}{\omega_1 + \omega_2} + \frac{\rho US}{2m}(-C_{z_\alpha} - C_D)]4I_x/\rho USd^2 \quad (4.0.1\text{-}6)$$

where the drag coefficient and lift curve slope must be obtained by other means. The drag coefficient, $C_D$, determination is straightforward - being proportional to the force required to prevent the model from moving along

the tunnel axis. This force is easily determined to a high level of accuracy from the currents in the coils. The slope of the lift coefficient, $C_{z_\alpha}$ (as well as other translational aerodynamics) can be obtained from a standard swerve reduction program[5] (proportional to the lateral distance traveled).

The useful part of the application of the quadricyclic solution to both transient and steady-state data lies in the ability to write either the real or imaginary part of the solution; e.g.

$$\beta = Re(\Delta) = K_1\cos(\omega_1 t + \phi_1) + K_2\cos(\omega_2 t + \phi_2) + K_3\cos\omega_3 t + Re(K_4) \quad (4.0.1\text{-}7)$$

and still have all the information contained. This enables the application of the techniques indicated to data from a single plane.

4.0.2 The second model to be considered is the fitting of the observations to the equations of motion using a technique which we will call the "Brute-Force" method.[7] For an axisymmetric model only the z force and M pitching moment equations are necessary for the inversion; however, data on all kinematic variables is needed:

$$wC_{z_w} + qC_{z_q} + pvC_{z_{pv}} + DwC_{z_{Dw}} + pDvC_{z_{pDv}} + prC_{z_{pr}} = \mu(Dw - qu + pv) \quad (4.0.2\text{-}1)$$

$$wC_{m_w} + qC_{m_q} + pvC_{m_{pv}} + DwC_{m_{Dw}} + pDvC_{m_{pDv}} + prC_{m_{pr}} = i_B Dq - (i_C - i_A)pr + i_E(p^2 - r^2) - i_F(qr - Dp) + i_D(qp - Dr) \quad (4.0.2\text{-}2)$$

where v, w, p, q, r are the nondimensional kinematic velocities and the i's are moments and products of inertia. This model is fitted by reduction to a set of algebraic equations as described below.

4.0.3 The third model is a specialization of the first one (eq. 4.0.1-2) Here only steady-state motion is considered, perhaps the most unique model for[2] free flight facility to be using. The advantage to steady-state reduction is, of course, the increased accuracy to which the data can be determined, having many cycles of data to "smooth" over.

4.0.4 The last model considered is the full six degree of freedom equations of motion given in reference 5. Here the motion is allowed to include nonlinear aerodynamics as well as nonlinear inertia terms.

## 5.0 Data Reduction Techniques

Three conceptually different classes of methods have been investigated for extracting aerodynamics from available observations. These three classes are referred to here as

1. Differential Correction Methods,
2. "Brute Force" Method, and
3. Steady State Analysis Method.

Most conventional procedures belong to class (1). Our particular adaptations are in some aspects unique, as will be explained below, but in general represent the state-of-the-art of this approach. Classes (2) and (3) are original approaches growing out of our research efforts at U.Va.

### 5.0.1 Differential Correction Methods

Here we are referring to the class of numerical methods which successively improve preliminary values for the unknown parameters in a given mathematical model until the computed output agrees with observations in some optimum sense (in our case, minimizing the weighted sum of squares of observed-minus-computed residuals). We have employed two differential

correction formulations in our data reduction analyses, these are

$$\Delta P = (A^T W A)^{-1} A^T W \Delta \Psi, \tag{5.0.1-1}$$

and

$$\Delta P = -\left(\frac{\Delta C}{G^T G}\right)^{1/2} G \tag{5.0.1-2}$$

where

$$\Delta P \equiv n \times 1 \text{ matrix of corrections to parameters,} \tag{5.0.1-3}$$

$$\Delta \Psi \equiv m \times 1 \text{ matrix of observation residuals,} \tag{5.0.1-4}$$

$$A \equiv m \times n \text{ Jacobian matrix of partial derivatives of the } m \text{ observables with respect to the } n \text{ parameters, evaluated with the current parameter estimates,} \tag{5.0.1-5}$$

$$W \equiv m \times m \text{ weighting matrix,} \tag{5.0.1-6}$$

$$\phi \equiv \Delta \Psi^T W \Delta \Psi, \tag{5.0.1-7}$$

$$G^T \equiv \left[\frac{\partial \phi}{\partial p_1}\Big|_c \bullet \bullet \bullet \frac{\partial \phi}{\partial p_n}\Big|_c\right] \tag{5.0.1-8}$$

and

$$\Delta C \equiv \Delta P^T \Delta P, \ \Delta C \text{ assigned empirically.} \tag{5.0.1-9}$$

The reader is referred to reference 8 for theoretical derivations and discussions of (5.0.1-1) and (5.0.1-2).

The first differential correction formula (5.0.1-1) is the classic least squares solution. The second formula (5.0.1-2) is the method of gradients ("steepest descent") solution for minimizing an arbitrary function.

Evaluation of the derivative matrix (5.0.1-5) is often a source of numerical difficulty. For analytic algebraic observation equations, we have developed, and used extensively a computer program which completely automates the process of partial differentiation. This process was employed with the quadricyclic solution as given in 4.0.1. For those cases in which the full six-degree-of-freedom equations (4.0.4) were integrated, we adopted a process known as parametric differentiation for computation of the elements of the observation Jacobian (5.0.1-5). This procedure[8] develops a set of m x n differential equations (one for each element of A) which can be integrated simultaneously with the equations of motion. These equations follow from straight forward partial differentiation of the equations of motion.

Comparing the method of gradients correction equation (5.0.1-2) with the least square correction equation (5.0.1-1), we note that use of (5.0.1-2) eliminates the necessity of inverting $(A^T WA)$, but introduces the necessity of controlling convergence rate by logically assigning $\Delta C$ (5.0.1-9) in (5.0.1-2). Our experience indicates that (5.0.1-2) is a valid alternative to (5.0.1-1), but should be employed only in the event that $(A^T WA)$ is so poorly conditioned that numerical inversion is impossible. We have found that the classical least square solution is typically an order of magnitude more efficient as the basis for least square differential corrections.

5.0.2 The "Brute Force" Method

Equations 4.0.1-1, 2 are solvable by differentiating the data numerically (using a five point central differencing scheme) and assuming all the observable kinematics to be known quantities. Thus the equations of motion are reduced to a set of linear algebraic equations in the aerodynamics which can be inverted to obtain the aerodynamics. As one might suspect, the accuracy of this method is highly sensitive to errors in observed data, since

numerical differentiation is being performed. This method also requires data on both position and angles in two orthogonal planes, however it is capable of handling a more sophisticated (i.e. nonlinear) model of the aerodynamic forces and moments.

For more details on this "Brute Force" method see reference 7. Comparison of this method with the others will be presented below.

5.0.3 Steady-State Analysis

5.0.3.1 Equations

As stated before, the coupled, complex, second order, linear differential equations which describe the motion of our model reduce to two complex algebraic equations when only the steady-state response is considered.

The resulting equations can be arranged[9] in the following fashion:

$$\text{Real} \quad \left(\frac{2\mu i\omega\Delta_o}{A_o}\right) \doteq [\hat{p}_o(C_{z_{pr}} + C_{z_{p\dot{\beta}}})]\omega + [C_{z_\alpha}] \qquad (5.0.3.1\text{-}1)$$

$$\text{Imag} \quad \left(\frac{2\mu i\omega\Delta_o}{A_o}\right) \doteq [-(C_{z_{\dot{\alpha}}} + C_{z_q})]\omega + [-\hat{p}_o C_{z_{p\beta}}] \qquad (5.0.3.1\text{-}2)$$

$$\text{Real} \quad \left(\frac{M}{A_o}\right) \doteq [-i_B]\omega^2 + [\hat{p}_o i_A]\omega + [-C_{m_\alpha}] \qquad (5.0.3.1\text{-}3)$$

$$\text{Imag} \quad \left(\frac{M_o}{A_o}\right) + \frac{C_{z_\alpha}}{2\mu}(i_A\hat{p}_o - I_B\omega) \doteq [-(C_{m_q} + C_{m_{\dot{\alpha}}})]\omega + [-C_{m_{p\beta}}\hat{p}_o] \qquad (5.0.3.1\text{-}4)$$

The terms appearing on the left hand side of the equations are all observables (or in the case of the last equation - computable before they are needed). These quantities are determined for each of several frequencies on the frequency response curve. Due to the periodic non-damped nature of the steady state solution $\Delta_o$ and $A_o$ can be determined using a simple least square procedure or fourier analysis to obtain amplitude, phases, and frequencies. Since a linear model has been assumed, observations of one plane of data (both angle and velocity) is sufficient. Each of the first four equations are valid for the n-points used on the frequency response curves. Therefore, we have n sets of equations whose solution is a simple non-iterative least squares reduction for the coefficients.

The major advantages of this method are its simplicity (no interation necessary) and its relative insensitivity to reasonable measurement errors.

The determinable coefficients include all of the coefficients on the right hand side of equations 5.0.3.1-1, 2, 3 and 4. This, it should be noted, includes inertia terms.

5.0.3.2 Magnetic Investigation of Resonance

In the steady state case the use of an oblate spheroid for the support element will also allow for an investigation of a resonance curve. In the previous section this was shown to be sufficient to determine the models aerodynamics. Use of an oblate spheroid provides an additional "spring constant" term (which is proportional to the magnitude of the main field) in the rotational equation of motion.

For discussion's here we assume no translation, the models motion is given by:

$$\{-[C_{m_\alpha} + C_{m_{\Delta_{BAL}}} + C_{m_{\dot\alpha}} D + i\hat{p}_o (C_{m_{p\dot\beta}} D)] + i_B D^2 - C_{m_q} D - i\hat{p}_o (I_A D - C_{m_{pr}} D)\} = M_o e^{i\omega\hat{t}}$$

(5.0.3.2-1)

Assuming the steady state solution ($\Delta = \Delta_o e^{i\omega\hat{t}}$ and for simplicity assume $\hat{p}_o = 0$, then rearranging and separating the equation into real and imaginary parts;

$$\text{Real } \left(\frac{M_o}{\Delta_o}\right) = -C_{m_{\Delta_{BAL}}} + [-i_B\omega^2 - C_{m_\alpha}] \qquad (5.0.3.2\text{-}2)$$

$$\text{Imag } \left(\frac{M_o}{\Delta_o}\right) = (C_{m_q} + C_{m_{\dot\alpha}})\omega \qquad (5.0.3.2\text{-}3)$$

For numerous runs, all with the same $\omega$ but different $C_{m_{\Delta_{BAL}}}$ the problem becomes the same as that described in the previous section. It should be noted that the "variable" is now $C_{m_{\Delta_{BAL}}}$ not "$\omega$" as before.

This method will be investigated numerically in the near future, no results are as yet available.

A disadvantage of this method that is that the translation equation of motion is unchanged. All the quantities appearing are constant, making it necessary to vary $\omega$ (as well as $C_{m_{\Delta_{BAL}}}$) to evaluate all of the aerodynamic coefficients involved.

## 6.0 Numerical Results

A comparative numerical study of how observational statistics propagate through the data reduction methods into statistics of the determined aerodynamic derivatives has been carried out. Observations were simulated by corrupting perfect (computed) values of the observables by adding Gaussian random relative errors. Several noise samples were taken at each noise level ($\sigma$); and each of the several applicable data reduction techniques were employed to determine the corresponding values for the aerodynamic derivatives. From these results, small sample statistics of the determined derivatives were computed for each method. Typical results of these analyses are displayed in figures 6, 7, 8 and 9 for a 15° included angle cone.

All the data are presented as percent standard deviation of the aerodynamic coefficients versus percent random noiset superimposed on the data. The major observation to be made is the consistent superiority of the steady-state method over the others. The translational derivatives (not shown) follow the same pattern with the steady-state method yielding the most accurate inversion at a given noise level. The errors noted in the differential correction methods are approximately the same as other investigators using these methods have found them to be.

One interesting fact to be reported on in detail in a future publication is the ability to separate $C_{m_q}$ and $C_{m_{\dot\alpha}}$ for reasonable noise levels using the "Brute Force" method.

† Curves 1 and 2 have a slightly higher positional noise level than the others, however our experience indicates that the moment coefficients are not extremely sensitive to positional noise.

## 7.0 Conclusions

An analysis of several methods for obtaining aerodynamic coefficients from the U.Va. superconducting magnetic suspension and balance wind tunnel system has been carried out. The method for inverting steady state free-flight motion yields more precise aerodynamic coefficients than transient methods at the same measurement noise level.

## References


1. Zapata, R. N., Paper A, This conference proceedings.
2. Stephens, T. "The Electromagnetic Position Sensing System", Paper G, This conference proceedings.
3. Lapins, M. "Optical Data Acquisition for the Cold Magnetic Balance Wind Tunnel Facility" Masters Thesis UVA June 1970.
4. Bass, R. W., and Gura, I. "High Order System Design Via State Space Considerations" Preprint, JACC Conference, Troy, N.Y. June 1965 p. 311-318.
5. Etkin, B. Dynamics of Flight, John Wiley and Sons, Inc. 1959.
6. Murphy, C. H. Free Flight Motion of Symmetric Missiles," BRL Rept No. 1216, July 1963.
7. Ragunath, B. S. "Error Analysis in the Evaluation of Aerodynamic Derivatives from University of Virginia Wind Tunnel Cold Magneitc Balance System." Ph.D. Dissertation UVA, June 1971.
8. Junkins, J. L. "On the Determination and Optimization of Powered Space Vehicle Trajectories Using Parametric Differential Correction Processes" MDC Rept No. G1793, 1969.
9. Jancaitis, J. R. "Steady-State Data Reduction Technique for UVA Cold Magnetic Balance System" Unpublished UVA Report 1971.

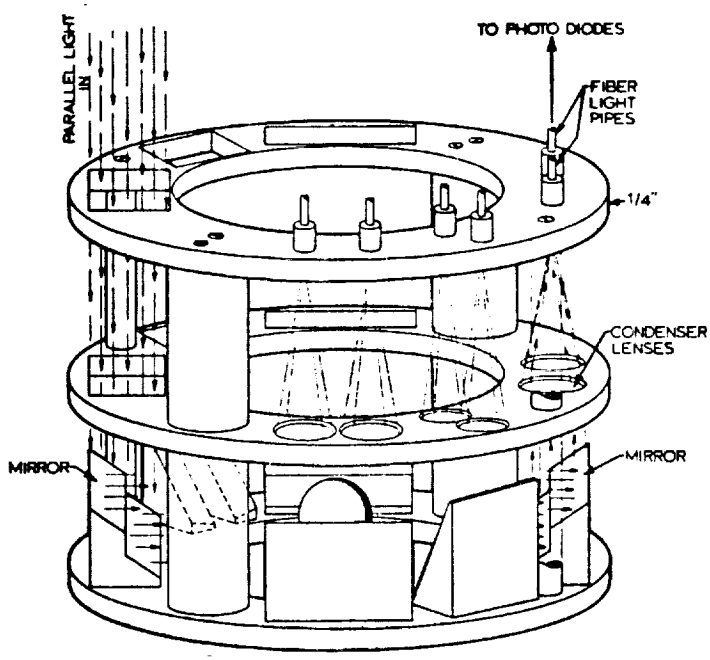


Figure 1 Optical Sensing System

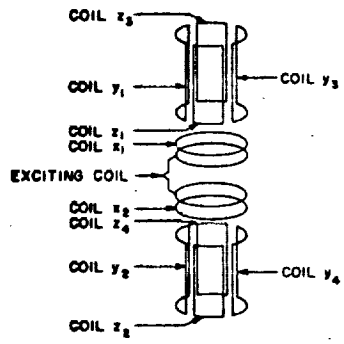


Figure 2 Electromagnetic Sensing System

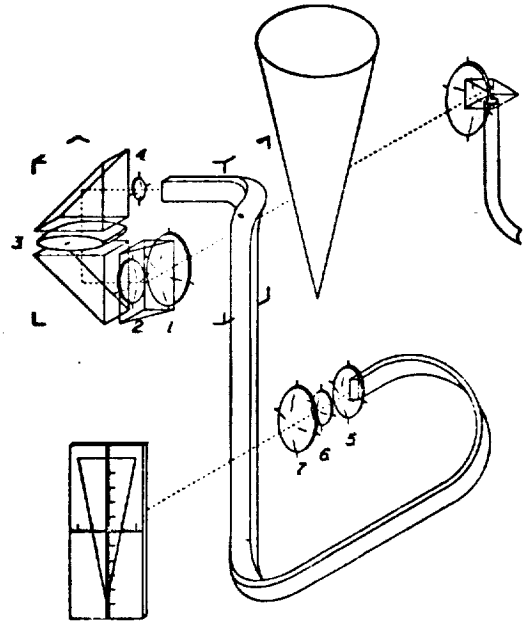


Figure 3 Fiber Optic System

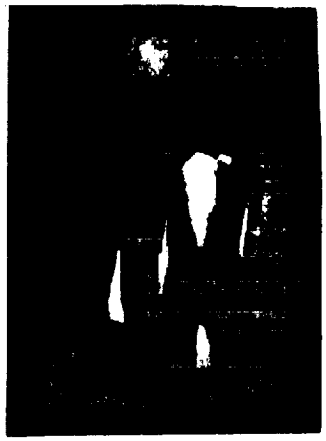

Figure 4 Distorted Cone

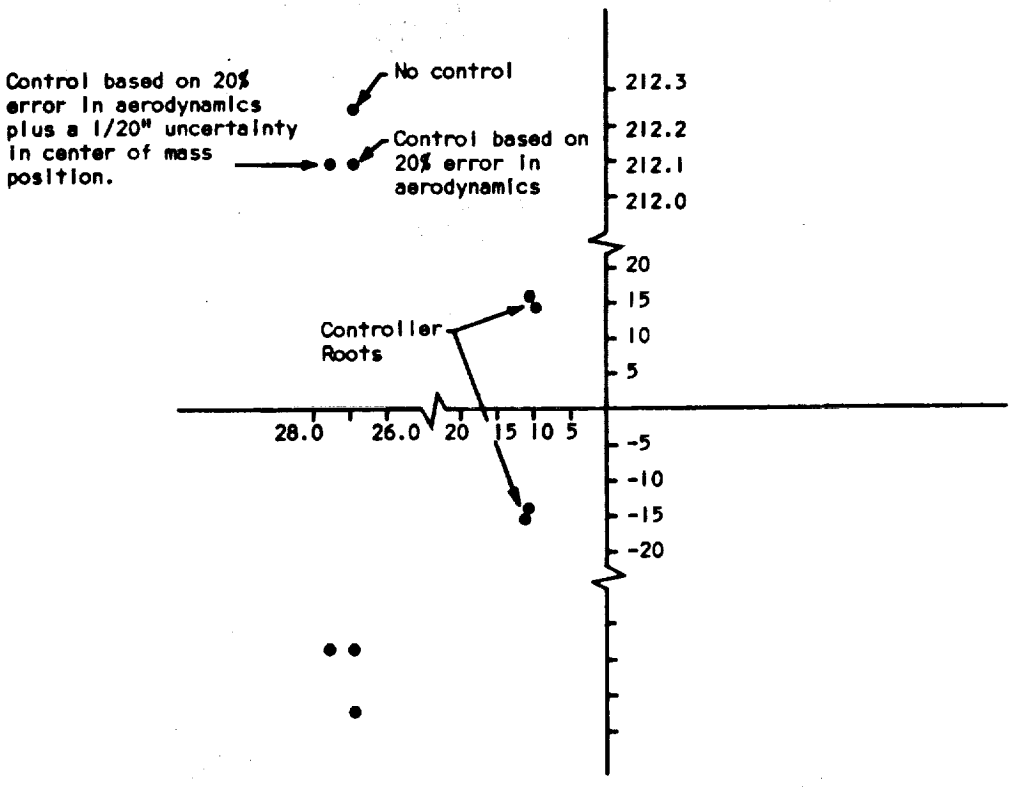


Figure 5 Root Locus of Model Aerodynamics

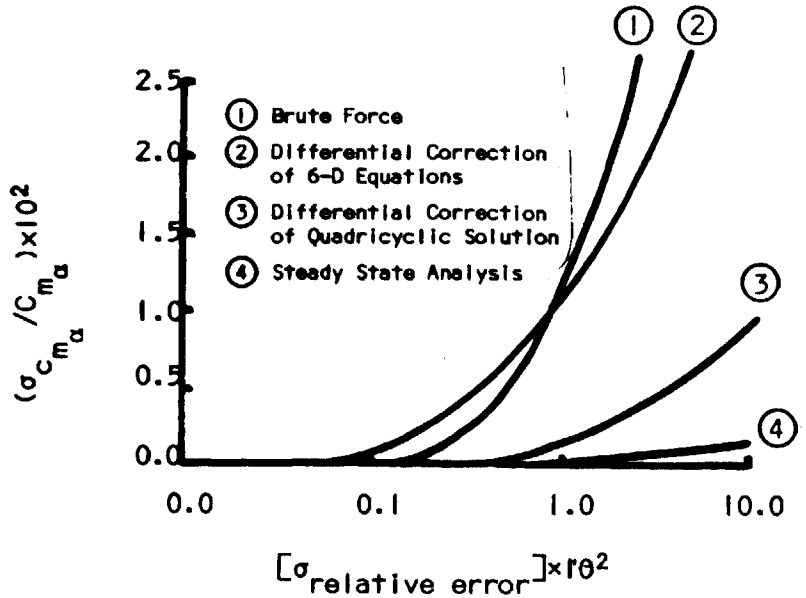


Figure 6

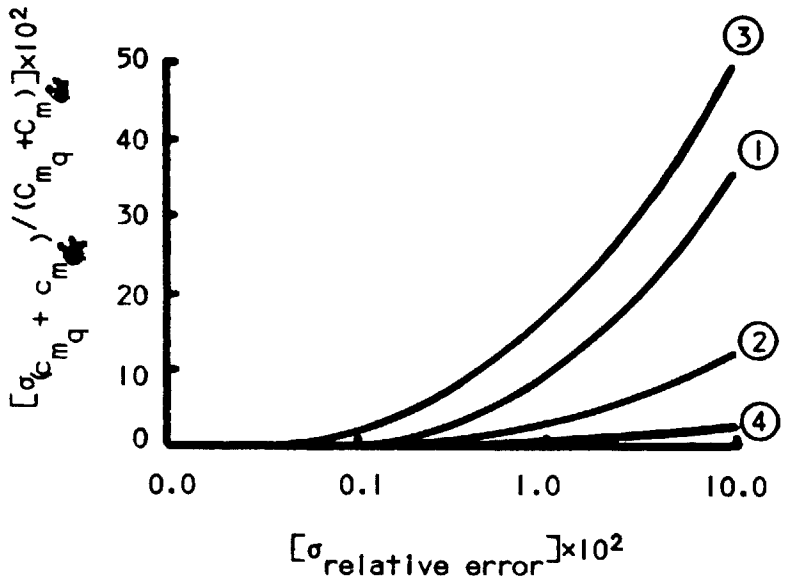


Figure 7

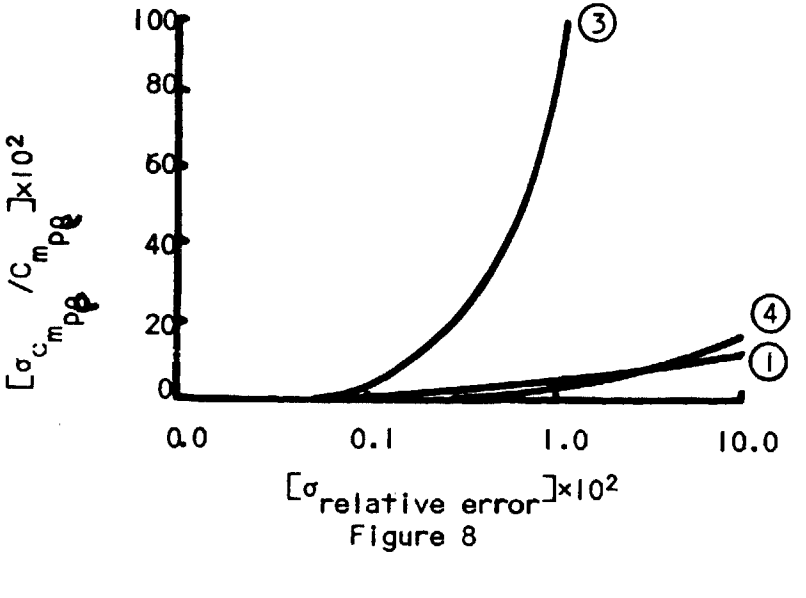


Figure 8

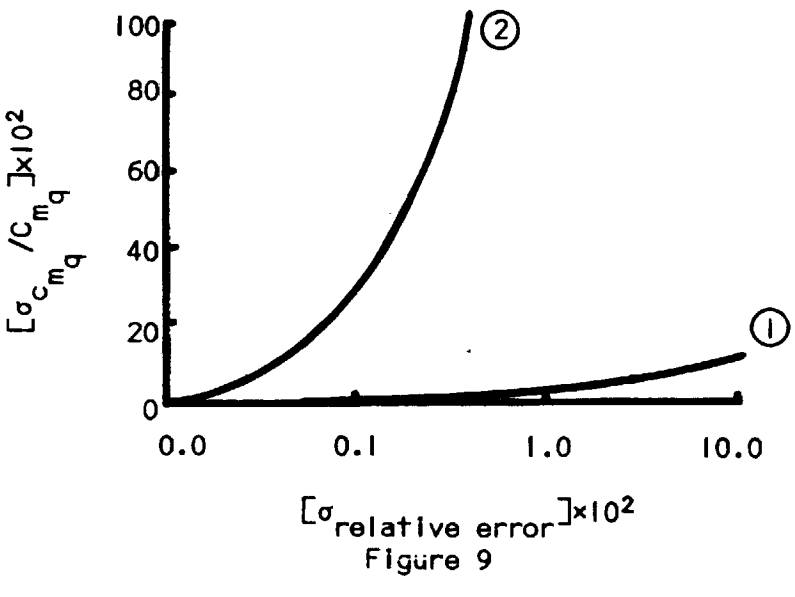


Figure 9

# THE USE OF IRON AND EXTENDED APPLICATIONS OF THE UVA COLD BALANCE WIND TUNNEL SYSTEM*

H.M. Parker and J.R. Jancaitis
Department of Aerospace Engineering and Engineering Physics
University of Virginia, Charlottesville, Virginia USA

The prototype design of the University of Virginia Cold Magnetic Balance Wind Tunnel System, primarily for assured performance, is based on the use of ferrites for the magnetic support element and for the case of spinning missile configurations in supersonic flow. The extension of applicability to non-continuously spinning airplane configurations and to subsonic flow regimes would be highly desirable. The problems involved in these extensions are discussed. The possible use of iron for the magnetic support element, or some material reasonable equivalent, is found to be crucial. The existing theoretical evidence that iron may be used without penalty is summarized.

*This work has been supported by Grants NGR-47-005-029 and NGR-47-005-112

I think it is correct to say that the motivation, certainly the dominant motivation, to develop the U.Va. Magnetic Wind Tunnel Balance was the desire to produce a scheme to measure, with reasonable precision, those aerodynamic forces and moments on a model which occur due to the motion of the model relative to the reference equilibrium state. There seems to me to be some lack of consistency in the literature about the use of the phrases "static stability" and "dynamic stability". However, I suspect we all could agree that static derivatives may be measured in an arrangement which holds a model in a fixed position and a fixed orientation in a wind tunnel; and that the measurement of a dynamic derivative requires that the model move in some fashion with respect to the tunnel.

It would make a good story to say that observing the need of better experimental methods to study the dynamic stability characteristics of aeronautical vehicles, or models thereof, we, after long study, came up with the U.Va. system. It would make a good story, but it wouldn't be true. In actuality, in another project in which we were trying to develop a precision, magnetically suspended gyroscope we sort of stumbled onto a 3-D magnetic support system for nearly spherical magnetic bodies. When something new is found, it is most natural to ask, "Now where else can I use this?" Thus, I fear, is how the U.Va. system was born. Incidentally, we did not develop a precision magnetically suspended gyroscope but I still personally believe that someday there will be one.

In addition to the virtually exclusive concern with dynamic stability, another important idea was present from the first days. Our sponsor agreed with us that in the prototype a prime objective was to learn how, even how best, to scale the system to a larger, considerably larger, size. For example, it was this basic idea, coupled with the hard facts of life about how conventional water-cooled copper coil systems scale, that resulted in the decision to go superconducting. If there ever was to be a four foot, or an eight foot, or a sixteen foot U.Va. system (the prototype is somewhat less than six inch) we believed it would be a superconducting system.

The fact that the AC operation of superconducting coils was not well understood at the time (I suspect is still not well understood)and the fact that such a system is a complex job of engineering perhaps serve to justify the choice of the simplest and easiest possible dynamic stability case to prove the concept. Whether or not it was justified let me describe for you some of the prototype design characteristics, in particular those pertinent to the ideas I wish to discuss:

1) A supersonic flow regime was chosen so that the ratio of model size to tunnel size would be large. One of the basic scaling relations is that the ratio of aerodynamic forces to balance produced forces goes inversely or the first power of the scaling length, i.e., aerodynamic forces are proportional to projected areas and the balance forces vary as the volume of the support element. The choice of a specific Mach number (i.e. ~3) involved the economic fact that the tunnel had to be of the blow-down type and that we wished the largest run times for our limited air capacity.

2) Spinning, axisymmetric models, i.e. typical missile configurations, appeared to be the simplest and easiest case for a number of reasons.

a) Roll control is not required of the balance since aerodynamic roll stabilization is straightforward to achieve.

b) The typical oscillatory motion of spinning missiles in flight, and the fact that by design, and perhaps a little trickery, the frequency of these oscillations can be adjusted over a considerable range, results in a reduced lateral force requirement of the balance.

c) The motion of the "Quasi-six-degree-of-freedom operation" grew out of these considerations.

d) No matter what position and motion detecting system was to be used, it seemed apparent that missile configurations would be the easier detection case.

3) At the price of a very significant reduction in balance force capacity, the support element material was chosen to be a ferrite. The reason is very simple. At the time when the prototype design has to be frozen, it was not certain what the effect of magnetic rotational hysteresis on the aerodynamic information extraction process would be. In fact, the general problem of the extraction of aerodynamic information from experimental six-degree-of-freedom motion data had not been studied in any significant depth at that time. Therefore since it was certain that a ferrite would have a negligibly small rotational hysteresis effect (another legacy from the old gyro project) the choice of a ferrite for the magnetic sphere tended to maximize the probability of success of the U.Va. system scheme to study dynamic stability.

Those design choices were deliberate. I believe it is essentially correct to say that the following things were recognized at the prototype "freezing point":

1) Some, but not all, of the engineering problems which would arise

2) The desirability of extending the applicability to typical airplane configurations and subsonic flight, and

3) The importance of whether or not the use of iron for the support element imposes a significant penalty on the extraction of information and therefore whether or not the increased force capacity to be derived from iron can be used. Let me remind you that pure iron has at the same time the largest saturation magnetization and the largest rotational hysteresis of any substance. The former insures the largest possible balance force capacity and the latter causes the largest rotational hysteresis effect.

The point of the present paper is that recent theoretical studies indicate that, at the prototype scale, the use of iron does <u>not</u> penalize the extraction of aerodynamic information, specifically, with the same noise level in the motion data, aerodynamic coefficients are extracted in numerical experiments with essentially the same accuracy with and without the maximum iron rotational hysteresis. Therefore it appears appropriate to begin serious consideration of of extending the applicability of the U.Va. system to non-missile configurations and subsonic flight. In the remainder of this paper two items will be discussed briefly: (1) Some of the problems involved in the proposed extension of applicability, and (2) The evidence for the feasibility of using iron.

SOME PROBLEMS IN EXTENSION TO AIRPLANE CONFIGURATIONS AND SUBSONIC FLOW

In the extension to these applications some rather obvious changes in the physical situation occur and result in changes in system specifications A qualitative discussion follows.

1) Since airplanes do not normally fly in a continuously rolling mode (even in aerobatics a continuously rolling rate is relatively small) it is evident that a non-continuously rolling mode is required. Therefore (omitting the consideration that some day a wind tunnel operator may literally fly his model in the wind tunnel via manipulation of aerodynamic control surfaces) it is evident that the system must provide roll control sufficient to cause only oscillation about some equilibrium roll position. Questions of whether the control is active or passive and how tight it must be depend upon future experiment for their answer. Two general sorts of things may be said. First, we at Virginia certainly hope that our friends here, or in France, or at MIT or somewhere will have found a nice roll control solution that we can simply copy. Second, it can be hoped, even expected, that a roll control system will be completely, or nearly completely, independent of the main system. (Like the Hungarian as a friend, we don't need another complication in our system!) It would appear that the roll control requirements are not essentially different in the supersonic and subsonic flow cases unless it is sensitive to the ratio of model size to tunnel size.

2) A second problem is termed the problem of balance force capacity and can be illustrated in the following way. Assume a given, fixed size system, and a given maximum gradient that it can produce at the support position. The balance force on the support sphere is proportional to the product of the magnetization of the sphere, the sphere volume, and the magnetic field gradient at the sphere position. On the other hand, the aerodynamic forces are proportional to a characteristic area of the model. In going from a missile configuration in supersonic flow to an airplane configuration in the same supersonic flow, the models probably will have nearly the same characteristic size, say the model length. Due to the difference in missile and airplane configurations, it is likely that the size of sphere that the airplane model could accommodate would be somewhat smaller than the size which the missile model could accommodate. Thus one expects the ratio of maximum support force to aerodynamic force to decrease somewhat, but not drastically, in going from a missile in supersonic flow to an airplane in the same supersonic flow.

Now consider the second stage, i.e. going from an airplane configuration in supersonic flow to an airplane configuration in subsonic flow, still with the same fixed system. In order to have an acceptably small tunnel wall interference effect, there must be a drastic decrease in model size, approaching an order of magnitude in the scale. Some relief can be expected in the reduction in q on going from supersonic to subsonic flow. However, if one admits the compressible subsonic ranges and an increased desirability to test at more realistic reynolds numbers, the q relief is not very large. Thus in extending to anything like ideal airplane in subsonic flow test conditions there is a rather drastic reduction in the ratio of maximum balance support force to aerodynamic force. Therefore those extensions,

especially the extension to subsonic flow, will require a rather drastic increase in the product of sphere magnetization and maximum magnetic field gradient. The fast magnetic field gradient is the difficult and expensive thing to produce; the sphere magnetization can easily be increased by going from a ferrite (saturated magnetization about 600 gauss) to iron (saturated magnetization about 20,000 gauss). The latter will be feasible provided that the use of ion does not impose too great a penalty on the end product of the whole operation, the extraction of aerodynamic information.

3) A third problem is related to the necessity of confining the model to some appropriate volume in the tunnel test section. Airplane configurations typically have much larger lateral (lift) force coefficient slopes than do missiles, certainly than the 15° cone that we have been considering. Thus for the same angular oscillation amplitude at the same frequencies the airplane configuration would experience much larger (in the ratio of the lateral force coefficient slopes approximately) lateral excursions of the model center of mass. Since any prospect of having the balance suppress these lateral oscillations of the model at these frequencies is too difficult and expensive to contemplate, i.e., the notion of Quasi-six-degree-of-freedom operation still holds, apparently the only reasonable solution is to arrange that the oscillation frequency is sufficiently high to produce an acceptable ratio of angular amplitude to translational amplitude. For a simple model in which a lateral force is proportional to the angular displacement, the ratio of translational to angular amplitudes goes inversely as the square of the frequency. Fortunately, it is easy to increase the frequency at which the model oscillates by use of a prolate spheroid of homogeneous, uniform magnetic material or its magnetic equivalent. This easy solution to the lateral containment problem will have a number of secondary effects which are not considered to be very important, e.g. less accuracy in observing the model motion, a reduced maximum driving capacity at the larger oscillation frequency, etc. One result, that the range of test reduced frequencies is significantly increased, may have more import than the authors realize.

It thus appears that the two major requirements associated with the extensions to airplane configurations and subsonic flow are (1) an adequate roll control system and (2) sufficiently increased fast balance force capacity. The roll control problem for the U.Va. system appears to be a straightforward one, in which good engineering, cleverness, etc. would appear to pay off substantial dividends. Indeed, it is hoped that it will only be a problem of adapting an existing system. In contrast, the problem of producing considerably larger fast force capacity presents the possibility of drastically different solutions corresponding to vastly different levels of cost. Let's put it this way. Assume NASA has made the decision to build an eight foot subsonic SMSB facility to study airplane configurations (and we think NASA just might some day). Imagine two design routes. In one ferrites are to be used and the fast force capacity is obtained by providing adequate magnetic field gradients at the support point. In the other design route iron is used for the support element and a correspondingly smaller magnetic gradient is required. Let us attempt to compare costs of the SMSB itself, i.e., coils, dewars, detection systems, power supplies, and excluding the wind tunnel, bldg., etc. Our rough, top-of-the-head estimate might be

$$\frac{\text{Cost, the ferrite way}}{\text{Cost, the iron way}} \sim \frac{5}{1} \text{ to } \frac{10}{1}$$

and we think we're talking about differences of several millions of dollars for and eight foot facility. Though we must warn you that these numbers cannot be taken literally, we do hope to impress you with the fact that we are convinced that the feasibility of the use of iron is a very important question.

## THE EVIDENCE FOR THE FEASIBILITY OF USING IRON

There are two phenomena involved in using, say, a sphere of pure iron for the support element. First, there is the eddy current effect. If the iron sphere is in a uniform magnetic field and is rotating about an axis which is not parallel to the field, eddy currents are induced in the sphere which interact with the magnetic field and produce a torque on the sphere. This induced eddy current torque (1) tends to decrease the angular speed and thus is partly dissipative and (2) tends to precess the spin axis toward the magnetic field direction. The magnitude of the torque is proportional to the angular speed, i.e. is a viscous torque. Fortunately, the eddy current problem is easily solved by any one of several methods of compositing the iron, which result in the bulk electrical conductivity being reduced by several orders of magnitude.

Secondly, there is the rotational hysteresis effect. If the iron sphere is rotated about an axis which is not parallel to the magnetic field, the induced magnetization is dragged along by the iron or lags behind the magnetic field. The $\vec{M} \times \vec{B}$ torque, due to this quite small lag angle between the magnetization and the external magnetic field, also has a dissipative component and a non-dissipative, erecting component.This has two characteristics which are important for our consideration. First, there is no known way of avoiding the rotational hysteresis effect. Second, the magnitude of the torque is independent of the angular velocity with which the sphere spins, and thus is a Coulomb type frictional effect. Additionally, for a given material, it depends on the magnetization, exhibiting a maximum at some intermediate magnetization and approaching a constant non-zero value at saturation.

The theoretical or numerical experiments to investigate the effect of the rotational hysteresis were done in the standard fashion. Perfect motion data is calculated, is corrupted with noise, and the noisy data is reduced to recover the aerodynamic parameters originally used. A comparison of the recovery accuracy vs. noise level relation for cases of with and without rotational hysteresis indicates the effect of rotational hysteresis on aerodynamic information extraction.

The model chosen is the same 15° cone, the anticipated first U.Va. model, used in other data reduction studies. To set the problem and to calculate the perfect data the following assumptions and approximations were made:

(1) body axisymmetric, both inertially and aerodynamically

(2) constant roll rate and constant x velocity, thereby reducing the problem to the lateral rotational and translational problem

(3) Linearized in the lateral angular displacements and the lateral translational and angular velocities ($\psi$, $\theta$, q, r, $V_y$, $V_z$).

(4) the conventional complex lateral plane formulation is used

(5) only steady state motion due to a driving moment is considered.

With these conditions the equations of motion take the form

$$A\dot{\gamma} + B\gamma + C\dot{\eta} + B\eta = 0$$

$$\ddot{\eta} + E\dot{\eta} + F\eta + G\dot{\gamma} + F\gamma = M_{ext} + R$$

where

$\gamma = \frac{V_z}{U_o} - i\frac{V_y}{U_o}$ is the complex velocity of the center of mass.

$\eta = \theta + i\psi$ is the complex angular displacement.

A,B,C,E,F,G are complex constants containing the aerodynamic coefficients and other parameters.

$M_{ext}$ is a non-dimensional external driving moment, and

R is the non-dimensionalized rotational hysteresis torque.

The rotational hysteresis term, R, is non-linear and is formulated in the following way. Define a unit vector $\vec{n}$ to be parallel to the x axis in the inertial, tunnel fixed reference frame and therefore parallel to the external magnetic field, $\vec{B}_o$. $\vec{n}$ may be written in terms of components in the body fixed reference frame. $\dot{\vec{n}}$, the time rate of change of $\vec{n}$ as observed from the body frame, may be calculated. In the approximation that the lag angle, $\delta$, by which the magnetization lags the external field, is small compared to the magnitude of $\eta$, the direction of the rotational hysteresis torque is the same as $\vec{n} \times \dot{\vec{n}}$. As stated earlier, the magnitude of the torque is constant. Therefore one finds that

$$R \sim \frac{-\dot{\eta} + i\hat{p}_o \eta}{|-\dot{\eta} + i\hat{p}_o \eta|}$$

where $\hat{p}_o$ is the constant roll rate. If $M_{ext}$ is of the form

$$M_{ext} = M_o e^{i\omega\hat{t}}$$

The driving moment corresponds to a constant magnitude torque which rotates in the lateral plane at the frequency $\omega$. The steady state solution of the form

$$\eta = \eta_o e^{i\omega\hat{t}} \quad ; \quad \gamma = \gamma_o e^{i\omega\hat{t}}$$

where $\eta_o$ and $\gamma_o$ are complex constants, is easy to obtain. From these the "observable" quantities $\psi$, $\theta$, $V_y$, $V_z$ may be calculated as a function of $\omega$, i.e. typical response curves. For a single value of $\omega$, values of each of $\psi$, $\theta$, $V_y$ and $V_z$ are calculated at 100 points over 10 cycles of the oscillation. These values are taken as the perfect data.

The reduction of the data is a straightforward process and occurs in two phases. The sets of 100 points are least squares fitted to obtain an amplitude and the resulting response curves combined with known parameters are least squares fitted to analytic expressions of the solution to find best values of certain combinations of the aerodynamic coefficients. Five independent sets of noise are used to corrupt the data and the standard deviation of the error in a recovered parameter is taken as the significant result, and is the quantity listed in Table I. In these calculations the value of the rotational hysteresis torque used corresponds to the largest value of rotational hysteresis loss exhibited by pure iron and which occurs at an external field at about 12,000 gauss.

Table I summarizes the results. A comparison of cases I and III clearly indicates that the presence of the maximum iron rotational hysteresis effect imposes no significant penalty on the accuracy with which these combinations of aerodynamic coefficients may be extracted from motion data for this motion cas

One can conclude that the prospects are bright, that experimental tests will show that the use of a composited iron support element does not significantly penalize the extraction of aerodynamic information from the U.Va. system. The impact of such a result on the extension of applicability and the cost of a larger future system will be great. A high priority is assigned to such experiments.

TABLE I

| Noise Level Standard Deviation as % of Amplitude of "observable" | $C_{Z_\alpha}$ | $C_{Z_q} + C_{Z_{\dot{\alpha}}}$ | $\hat{P}_o C_{Z_{p\beta}}$ | $C_{m_\alpha}$ | $C_{m_q} + C_{m_{\dot{\alpha}}}$ | $\hat{P}_o C_{m_{p\beta}}$ | Case |
|---|---|---|---|---|---|---|---|
| 10 | .2 | 2.9 | 223 | 04 | .4 | 18 | I. No Rotational Hysteresis |
| 1 | .04 | .5 | 20 | .08 | .08 | 3 | |
| .1 | .02 | .02 | 1.1 | .07 | .02 | .2 | |
| 0 | .02 | .007 | .2 | .07 | .02 | .07 | |
| 10 | .15 | 3.8 | 71 | .6 | .5 | 46.6 | II. Rotational Hysteresis in data, reduced as if no Rotational Hysteresis |
| 1 | .04 | .4 | 10 | .3 | .08 | 46.6 | |
| .1 | .02 | .002 | 1.4 | .3 | .03 | 46.5 | |
| 0 | .02 | .007 | 0.5 | .3 | .03 | 46.5 | |
| 10 | .4 | 3.7 | 352 | .4 | .4 | 19.7 | III. Rotational Hysteresis in data, Rotational Hysteresis taken into account in reduction |
| 1 | .02 | .3 | 9.9 | .1 | .03 | 3.2 | |
| .1 | .02 | .04 | 1.3 | .1 | .004 | 3.5 | |
| 0 | .02 | .007 | .3 | .1 | .001 | 3.4 | |

Discussion

Mr. Stephens. Have you looked at some of these fancy magnetic materials like Supermalloy?

Professor Parker. It looked to me that iron has the biggest rotational hysteresis effect and the highest saturation magnetisation. Incidentally, I do not think that we are going to be able to take advantage of all of the saturation magnetisation because before that is reached we may run into troubles caused by too high a field on the superconductors.

# ELECTROMAGNETIC POSITION SENSOR FOR A MAGNETICALLY SUPPORTED MODEL IN A WIND TUNNEL

by

William R. Towler
Electronic Instrumentation Group
Research Laboratories for the Engineering Sciences
University of Virginia

## PURPOSE

An investigation was undertaken at the University of Virginia to determine the feasibility of using superconducting force-producing coils for positioning a model in a wind tunnel. The cryostat containing the forcing coils surrounded the test section of the tunnel, thus favoring an electromagnetic position sensor. Another reason favoring this choice was the fact that the performance of an electromagnetic sensor is essentially unaffected by the shape of the model.

As the research work was to be primarily concerned with the superconducting force coils and their drivers, and as the group at the Aerophysics Laboratory of the Massachusetts Institute of Technology had a sensor essentially completed, Dr. Timothy Stephens of M.I.T. kindly provided us in the summer of 1967 with drawings and details of his design.

A sensor was built based on the M.I.T. design as shown in the **figure number Q3.** The cylindrical form holding the coil assembly has a cylindrical opening of 15.24 cm in order to accommodate a lucite tube with an outside diameter of 14.92 cm in which the test model is placed. The entire coil assembly is 50.8 cm long.

## EXCITATION COILS

The excitation coil with a self inductance of 35.2 microhenries is split in two sections as shown in the slide and is located symmetrically with respect to the coordinate origin; the coil axis is coincident with the tunnel axis of the system. Parallel resonance was obtained by placing the resonating capacitors on the coil form, thus minimizing the current requirements from the power amplifier.

## PRINCIPLE OF OPERATION OF THE SENSING COILS

The sensor is based upon the principle of the differential transformer. Briefly, the operation is as follows: With reference to the slide, consider coils $x_1$ and $x_2$ as being two secondaries symmetrically located about the excitation coil. The model containing a ferromagnetic object is located midway between the two excitation coils and on the axis of the coil

of the current in one coil pair is reflected throughout the system.

After encountering these difficulties, a nonresonant arrangement was tried. An operational amplifier connected in a noninverting voltage follower mode was used on each coil pair as shown:

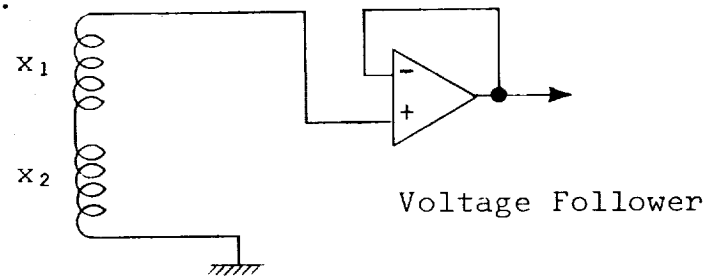


In this arrangement the amplifier appears as a 300 megohm load to the coil and the circulating currents in the coil are reduced until the cross coupling between coil pairs is essentially eliminated. Except for matching the coils in each coil pair to the nearest turn, no attempt is made to eliminate the signal produced by the slight unbalance until the signal has passed through the voltage follower and a 30 K Hz band-pass filter. Then, before amplifying and demodulating, the unbalance signal is cancelled with a signal from the excitation source. This nonresonant arrangement yielded an increase in sensitivity of about 3 fold over the first resonant arrangement, with no noticeable interaction between coils. During bench tests the sensitivity was sufficient to detect motions of the model as small as .001 cm without being troubled by noise. The sensor was placed in the cylindrical cavity through the cryostat. Sensitivity was reduced to approximately one-one hundredth of the original value because of the stainless steel lining, but this still left sufficient sensitivity above the noise.

However, the coup de grâce was administered by the power amplifiers that drive the superconducting force coils. The current is supplied to the superconducting coils in the form of triangular pulses whose rise rate is 25 amperes per millisecond. In the extreme case, the amplifiers introduce a current from zero to 350 amperes in 14 milliseconds. Each time any one of three power amplifiers introduces a current pulse, the entire sensor is overwhelmed and remains inoperative for the duration of the pulse. A narrow band 30K Hz filter was provided to reduce the effects of the power amplifier but it proved inadequate.

As the problems with this sensor appear rather difficult to eliminate, an optical sensor is now being used. We hope eventually to solve the problems encountered with the electromagnetic sensor and to be able to take advantage of its unique characteristics.

assembly. Coils $x_1$ and $x_2$ consist of many turns connected in series opposing, so there is no output voltage across the output of these two when the model is centrally located at its null position. If the model is displaced axially from this null position, the rate of change of flux from the excitation coil is no longer equal in $x_1$ and $x_2$; the two voltages induced in $x_1$ and $x_2$ no longer cancel and a net output voltage results. If the model moves toward $x_1$, the voltage in $x_1$ predominates; if the motion is reversed the voltage in $x_2$ predominates. The phase of the net output voltage when referred to the primary excitation is different by 180° in the two cases mentioned. This phase difference is used to determine the direction in which the model moves from null and the amplitude of the output is a measure of how far the model moves. Hence, coils $x_1$ and $x_2$ sense motion in an axial direction or in the X direction as shown on the slide. The other coils operate on the same principle to sense motion in the Y and Z directions. The voltages from the other coils can be used to sense pitch and yaw motions.

A conducting ring located in the model can be used as the sensed object as an alternate to the ferromagnetic material. The currents induced in the ring are always induced in a direction to oppose the flux being forced through the ring from an outside source. This principle reduces the flux in the proximity of the ring; an opposite effect is produced by a ferromagnetic object.

## RESULTS

The magnitude of the voltage induced across the secondary coils is the voltage across the primary multiplied by the ratio of the number of turns in the secondary and primary for unity coupling. This magnitude must, of course, be reduced by that fraction formed by the flux that links the secondary divided by the total flux produced by the primary. This fraction can be calculated by expanding the distance function in spherical harmonics or other series and then integrating over the area of the secondary coil. The results of these calculations show that the output is sufficiently large to be workable in any except rather extreme conditions.

In the early stages of development an attempt was made to resonate all the secondary coils at the frequency of the primary excitation. This approach ran into difficulties. For best performance, the resonating capacitors should be located as close as possible to the terminals of the coils, but space was a problem. Locating the capacitors outside the tunnel area involved using approximately a meter of cable for each coil pair. It was then found that the resonance was affected by the position of the connecting cables even though coaxial cable was used.

At resonance, each coil has circulating currents significantly large and therefore acts as another primary to the other secondaries. Under these conditions any change in the magnitude

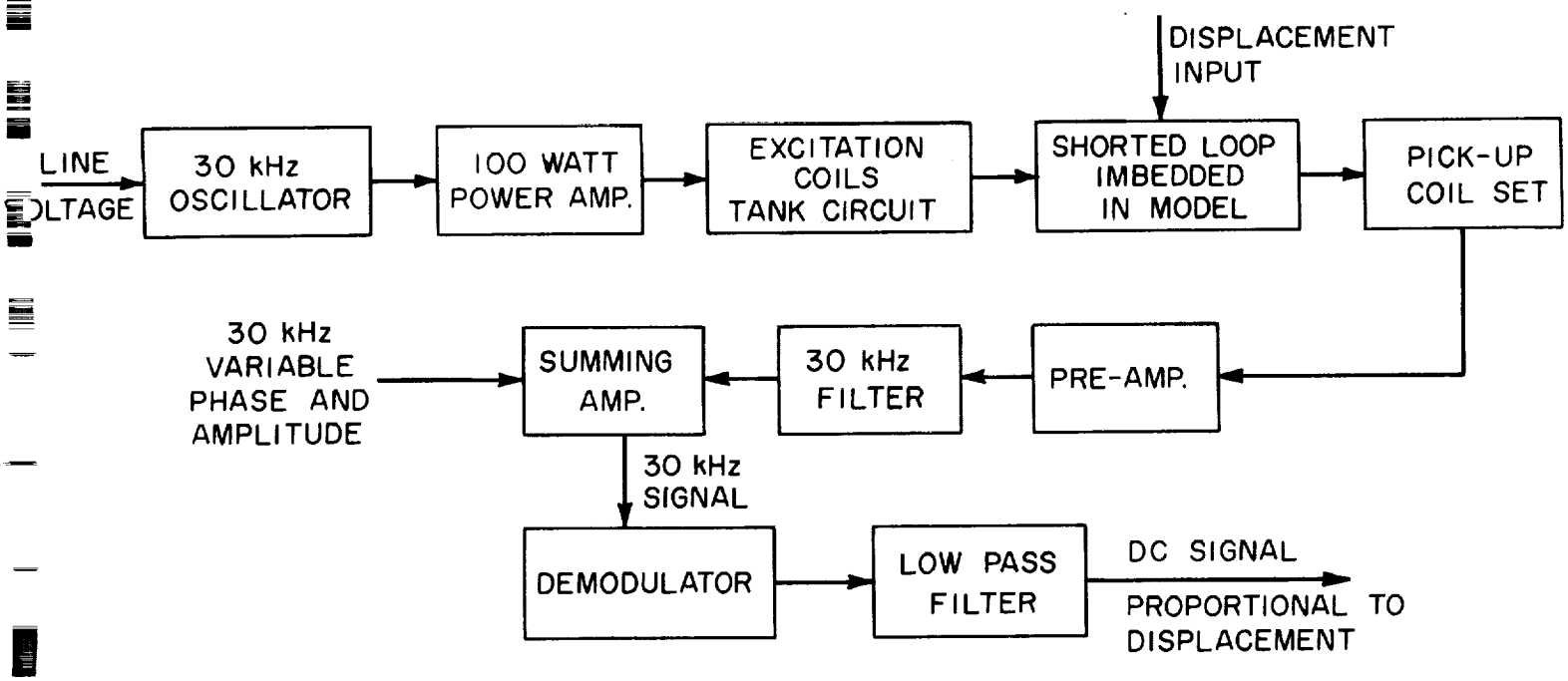


a) BLOCK DIAGRAM

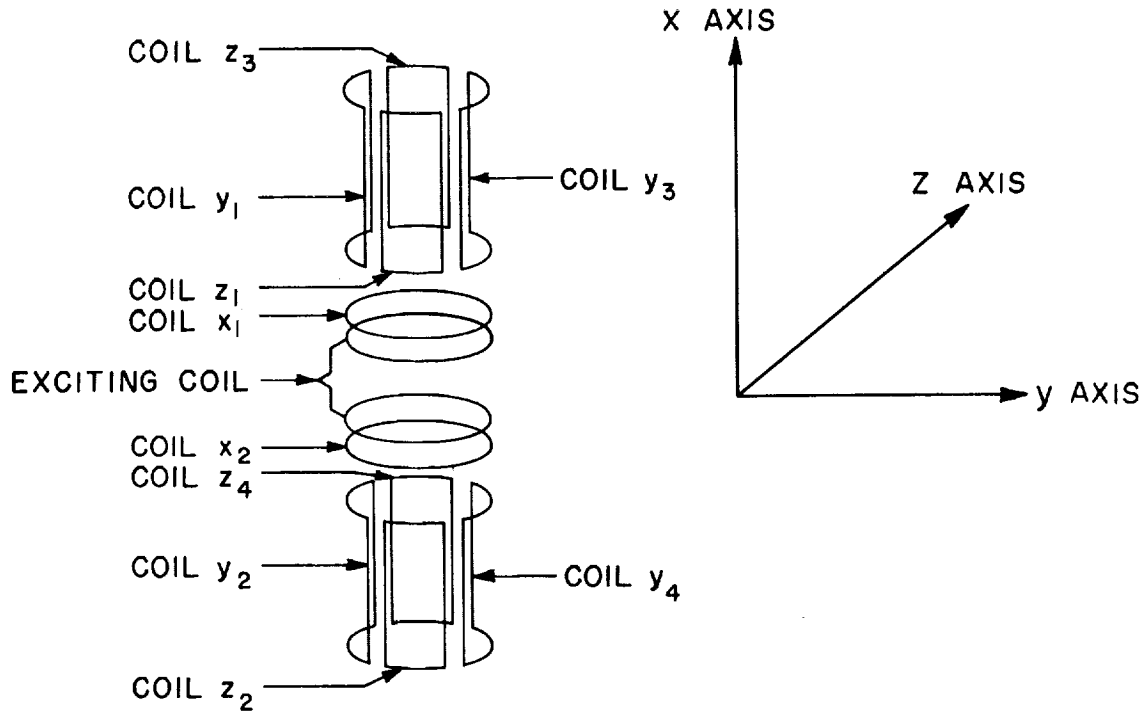


b) COIL ASSEMBLY

FIG. Q3

# SAFETY ASPECTS OF SUPERCONDUCTING MAGNETIC SUSPENSION SYSTEMS

by Professor R.N. Zapata

University of Virginia

You will appreciate that we have a combination in our system of a high energy store in the magnetic fields, inside a pool of liquid helium. There would not be enough liquid to absorb the energy if it was released. We have been concerned about safety, and have accumulated experience which we would now like to share with you. We have confidence that a system like this can be made very safe.

On Figure 2 of paper A you will see a cross section through our magnet and cryostat system. The system is shown in Figs. Q4 and Q5. The helium level is about at the lower radiation shield. We are concerned with energy stored in all nine coils. We have done things that are straightforward, like providing blow-off valves so that if the pressure rises due to rapid boil-off, the vapour can escape easily. The vapour cooled leads are connected to the main helium vapour manifold for the return of vapour. The connections are by flexible lines which would blow off very easily before any of the other hardware would blow. We also monitor temperature inside the cryostat so that we get very quick indications as a sound alarm if the liquid level drops. We also have a flow meter to tell us if the boil-off rate jumps. The main protection has to be done through the main power supplies. We have protections in all three supplies. The simplest power supply is that feeding the main field coil which is strictly a D.C. coil. What we have there is a pair of diodes across the output leads of the power supply. This has proved very effective. We have had occurrences such as adjusting the current or changing the coil too rapidly with the result that it went normal. It is pretty obvious that the flow rate went up rapidly. Nothing terrible happened in this case. We immediately cut the voltage of the power supply, but because of the presence of the diodes the coil was not damaged and we used it again five minutes later. We have a spark gap protection across the power supplies feeding the drag augmentation coils. We did not have this when we had our only accident with these coils. It may be interesting to hear a few details of this accident which was of a strictly mechanical nature. It was due to a poorly made coil former which failed when we put current to the drag augmentation coil at the same time that we had current through the main field coil. The repulsive forces were of such a magnitude that the upper drag augmentation coil former was sheared, Fig. Q6. The average stress was only 60 p.s.i., but nevertheless it did shear and the whole magnet system was separated, all this happening of course in a pool of liquid helium. The conductor was cut off and a lot of helium boiled off, Fig. Q7. The power supply was partially damaged, but no catastrophic failure occurred. The coil is just being re-wound so that all the experiments have since been performed with just the aid of the main coil.

The most important aspect of safety has to do with the main power amplifiers and the gradient coils. There is a great deal of power which we can handle very rapidly, being pumped in and out of the system. I think that Brown-Boveri did a very good job in providing a lot of safety devices

in the power supplies. At the beginning we could hardly turn them on because of the 10 or 15 interlocks. They are self protected in such a way that if one of the gradient coils fails and starts dissipating a lot of heat the power supply will cut itself off automatically, before we can even see the rise in the evaporation rate of helium.

I have shown you and discussed various forms of failure, so that anyone who is building a system should think of the kinds of safety problem that they could encounter. I believe that all of these things have contributed, although they have been a nuisance because you have to open the system and take a couple of days to rewind a coil, to giving us a great deal of confidence in how well you can handle a system which after all is completely new. We would like to ask anyone who has experience with superconducting systems and who has good suggestions on additional safety precautions that we might take to exchange experience with us.

## SECTION III

## SUMMARY OF PROGRESS SINCE JULY 1971

This final technical report would not be complete without a brief discussion of progress since July 1971, particularly in what concerns the unsettled questions about full operational status of the prototype facility. These questions were centered about two principal issues: (1) replacement of one gradient coil and one drag augmentation coil which had been severely damaged during preliminary testing of the facility; (2) final debugging of the control circuit.

The first issue was settled in two parts. Firstly, the Cryogenic Engineering Company (CRYENCO) finally agreed to build a drag augmentation coil form of improved design and pay the Superconductivity Laboratory at the University of Wisconsin for the rewinding of that coil. This work was completed at the beginning of 1972. Secondly, the gradient coil which had failed repeatedly during early tests was rewound with extreme care in our laboratory and tested individually before installing it in the facility. This work was completed at the beginning of the summer of 1972. Both coils performed satisfactorily during subsequent tests of the entire facility, thus demonstrating that no fundamental problems were involved in prior failures. The second issue was settled by building a water-cooled suspension system compatible with all other components of the prototype schedule for the rather complex control circuit. Successful three-dimensional stable suspension of a one-inch sphere in this auxiliary water-cooled system was achieved in June 1972, which demonstrated the viability of the control circuit design.

Finally, on July 22, 1972, stable three-dimensional suspension of one-inch spheres of two different ferromagentic materials was acheived in the prototype facility. This constituted an important milestone in the development of wind tunnel magnetic suspensions and confirmed our most optimistic expectations about the potential of superconducting tehcnology for large scale magnetic suspension systems.

At present, work is continuing with funding from NASA grant NGR-47-005-112. Full details of progress in this phase of the project will be reported at the end of the summer of 1973.

FIG. 9A

9/11

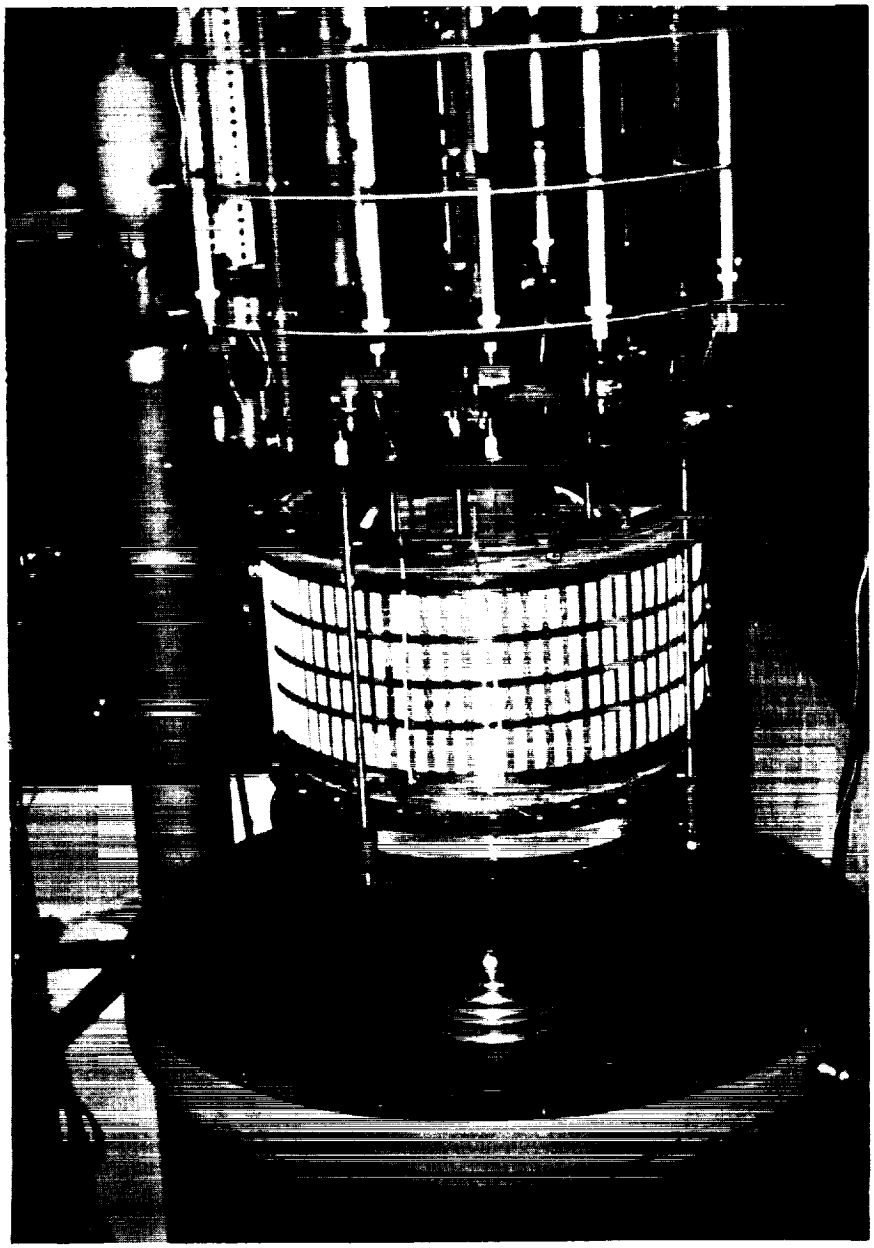

FIG. Q5

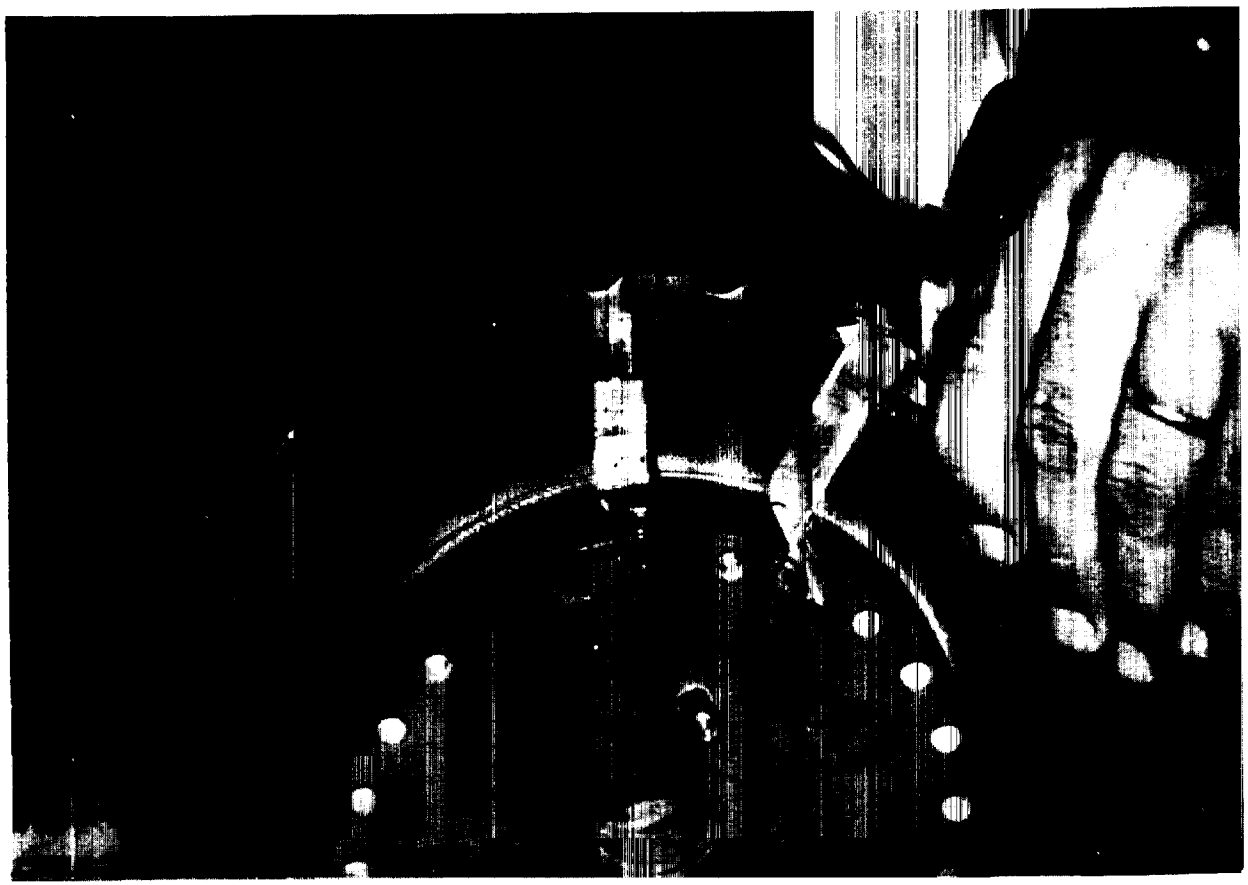

FIG. Q6

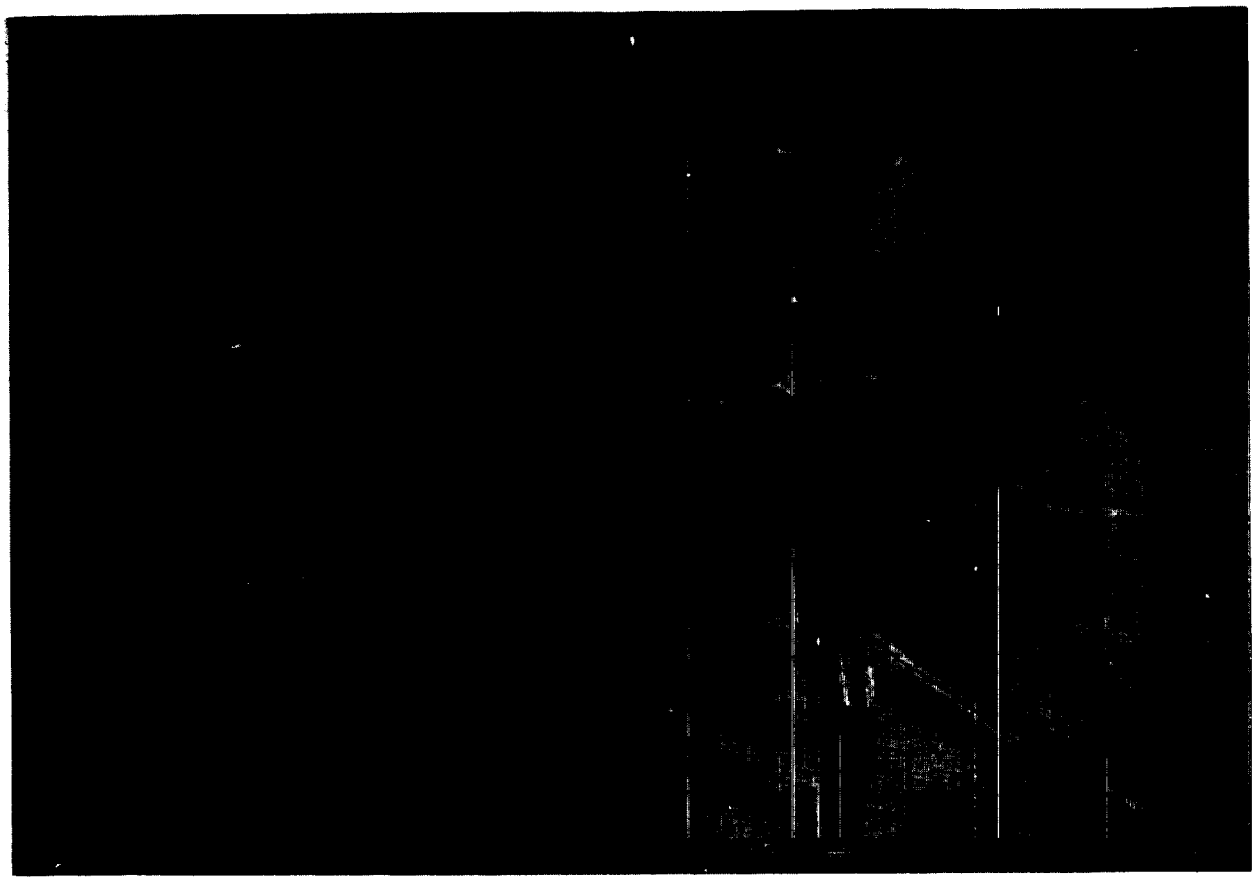

FIG. Q7

## REFERENCES


1. "Theoretical and Experimental Investigation of a Three-Dimensional Magnetic-Suspension Balance for Dynamic Stability Research in Wind Tunnels," Technical Annual Status Report No. AST-4030-105-68U, March 1968, by H. M. Parker, R. N. Zapata, G. B. Matthews.

2. Short progress report by H. M. Parker circa March 1969.

3. Letter request for supplemental funds and time extension, by R. N. Zapata, September 12, 1969.

4. Letter request for supplemental funds and time extension, by R. N. Zapata, October 15, 1970.

5. Proceedings of the Second International Symposium on Electro-Magnetic Suspension, published by the Department of Aeronautics and Astronautics, The University of Southampton, 1972.

DISTRIBUTION LIST

| Copy No. | |
|---|---|
| 1 - 5 | NASA Scientific and Technical Information Facility<br>P. O. Box 33<br>College Park, Maryland 20740 |
| 6 - 7 | Research Models and Facilities Division<br>Langley Research Center<br>Hampton, Virginia 23365 |
| 8 - 10 | R. N. Zapata |
| 11 - 12 | H. M. Parker |
| 13 | J. E. Scott, Jr. |
| 14 | R. A. Lowry |
| 15 | C. B. Thomas |
| 16 - 18 | RLES Files |